I. SPECTROMETER FOR ZERO-FIELD SPIN RESONANCE

II. TRIPLET EXCITON SPIN RESONANCE IN ZERO FIELD

Thesis by

Arthur William Merkl

In Partial Fulfillment of the Requirements

For the Degree of

Doctor of Philosophy

California Institute of Technology

Pasadena, California

1964

Meinen Eltern gewidmet

Die sich stets dafür geopfert haben,

dass ihre Kinder das Leben in völligeren,

Masse geniessen können.

ACKNOWLEDGMENTS

It is with a deep sense of gratitude that I acknowledge my debt to Professor McConnell. He has been an inspiring scientific advisor and a friend.

Thanks are due to other persons at the Institute, particularly fellow graduate students, who have made my stay here a memorable experience.

I am indebted to the National Science Foundation, to the Institute for Scholarships, and to the Atomic Energy Commission for the financial assistance necessary for my graduate study.

Finally I wish to thank Robert Metzger for his pains-taking critique of the first draft of this thesis.

TABLE OF CONTENTS

PART I

SPECTROMETER FOR ZERO-FIELD SPIN RESONANCE

A. INTRODUCTION

High Field -- Systems for the observation of electron spin resonance of paramagnetic substances in large magnetic fields generally consist of the following circuit elements: (a) a fixed-frequency, high Q*, radio frequency source, (b) a variable D. C. field electromagnet, (c) an A. C. magnetic field modulation system, (d) a detector, frequently a diode detector, and (e) a narrow band amplifier and lock-in detector.

In high field the frequency of the radio frequency source (generally a klystron) is locked to the natural frequency of a high-Q microwave cavity. The resonance is found by sweeping the large D. C. magnetic field. This D. C. field is generally modulated with a small A. C. field of frequency 400 cps to 100 kc/sec. Resonance absorption by the paramagnetic sample causes the radio frequency field to be amplitude modulated at the modulation frequency. This modulation is detected with a crystal, amplified, and then can be either directly observed on an oscilloscope or fed through a lock-in amplifier to a chart recorder.

ZERO FIELD -- Typical components for a zero-field electron spin resonance spectrometer are: (a) a variable frequency

---

*Q = quality factor = $\frac{\Delta\omega}{\omega}$ = $\frac{\text{energy stored in resonant circuit}}{\text{energy dissipated per cycle}}$

high-Q, radio frequency source of frequency independent sensitivity, (b) a region of zero D. C. magnetic field, (c) a modulation system, (d) a detector, and (e) an amplifier and lock-in detector.

The last four requirements are easily satisfied. In many experiments the earth's magnetic field causes only a small perturbation of the transition frequency and/or the line width. When the effect is large, either an arrangement of Helmholtz coils, or a large, judiciously placed permanent magnet will reduce the field over the sample region to almost any desired value. Suitable modulation and detection systems are described in Part I. C-2 of this thesis, so that no general comment is necessary at this point.

Since, however, the radio frequency oscillator is invariably the largest source of difficulty, a rather detailed general discussion will be presented before the specific design used in the present work is given.

B. RADIO FREQUENCY OSCILLATORS

In the following, only those problems are discussed which are likely to be encountered by anyone endeavoring to do electron spin resonance absorption work in the frequency range from about 10 to 3000 Mc/sec.* (Most of the ideas presented are applicable to the consideration of equipment design for nuclear magnetic and nuclear electric quadrupole resonance as well, if one allows for such differences as the variation in line widths.)

Zero-field electron spin resonance transitions occur over a wide frequency range, and their line widths (in frequency units) are often (a) as large as 10% of the resonance frequency, (b) comparable to the tunable range of the oscillator. This is especially true of broad transitions occurring below 100 Mc/sec(2).

The different electronic hardware used in oscillator circuitry allows us to divide the frequency range into several overlapping bands.

B-1. 10 to 125 Mc/sec -- This range is conveniently covered by familiar lumped-parameter circuitry. Air core radio frequency coils and variable tuning capacitors of a convenient size are used. At the higher frequency end of this range the distributed

*For a general treatment of the theory and design of electrical oscillators, see the texts listed in Reference (1).

capacitance and inductance of the oscillator components becomes an appreciable percentage of the total reactance needed, greatly reducing the tuning range. Careful choice of components (e.g., tubes with small interelectrode capacitances) and the actual layout of the circuit become critical.

Careful radio frequency shielding of all components, especially the coil, is essential. Commercial FM as well as amateur broadcasting in this range will cause spurious resonances in an improperly shielded oscillator.

The possibility of using coaxial lines, as described below, for at least part of this frequency range should be investigated. Three frequency-lowering devices, which would not affect the Q appreciably, are suggested: (a) the connection of additional capacitance in parallel with the tuning capacitor, (b) filling part of the coaxial line with a non-lossy dielectric, and (c) changing the relative diameters of the coaxial lines to obtain a lower inductance.

B-2. 125 to 500 Mc/sec -- Largely because of the inductive effects of even the shortest leads, it is almost impossible to use the above described lumped-parameter circuits at frequencies much above 125 Mc/sec. This is a transition range where hybrid circuits are used. Coaxial lines, less than 1/8 wavelength long, serve as inductive elements, and small butterfly

capacitors are used to tune the oscillator. Since all of the oscillator circuit components, including the tuning capacitor and vacuum tube, may be placed inside the coaxial line, we have a completely shielded oscillator. Under these circumstances there are no problems with stray radiation and radio frequency pickup.

A coaxial-line oscillator of this type was used in the observation of the higher frequency zero-field exciton resonance transitions in $(\phi_3 AsCH_3)^+ (TCNQ)_2^-$*, and a more complete description of the oscillator is given in Part I. C.

B-3. 500 to 3000 Mc/sec -- Above 500 Mc/sec the wavelength of the radio frequency radiation is sufficiently short that it is convenient to use resonant cavities. Although circular or rectangular cavities could be used, coaxial lines have found more application. There is, however, an important difference from the design in Part I. C-2 above. The coaxial lines used in this case are approximately either $n\lambda/2$ or $n\lambda/4$ in length. Actual resonant cavity modes are present, and there are maxima and minima in the electric and magnetic fields along the line. In the above case a sample could be placed anywhere in the grid coaxial line, the field being roughly equal throughout. In this case, however, the sample should be placed in a region of magnetic field maximum.

Because of transit-time problems (the time of flight for the

* TCNQ = Tetracyanoquinodimethane

electrons in the vacuum tube becomes non-negligible at these frequencies), only specially constructed vacuum tubes can be used in this region. The most readily available are the lighthouse tubes, which have a frequency range extending to ca. 3000 Mc/sec. Large power outputs are available (kilowatt continuous wave), which should be useful in saturation experiments. These oscillators are readily pulsed, and, therefore, even larger peak power output can be attained.

To operate these tubes continuously in a sensitive mode (marginal oscillation), circuit design should be such that the tubes are run at about 10% of their rated power. In this way, the tubes are run in a (roughly) linear region of operation, and the tube characteristics do not determine the level of oscillation in such a manner as to make the oscillator insensitive to small changes in loading (resonance absorption) of the tank circuit.

Super-regenerative oscillation is also quite sensitive to changes in cavity loading, and a super-regenerative oscillator used to detect the nuclear quadrupole resonance of Iodine has been reported (3). The Radiation Laboratory Series (4) of M. I. T. contains the most complete and readily accessible information on lighthouse tubes and oscillators covering this frequency range.

Two recently developed components, Nuvistor (5) tubes, and

tunnel diodes (6), are capable of operation in this frequency range. The power levels currently available, however, are quite small, of the order of milliwatts. A lack of familiarity with these elements precludes further comment, and they are mentioned only to provide a more complete picture of the components available for use in this frequency range.

C. ZERO-FIELD SPIN RESONANCE SPECTROMETER

A block diagram of the zero-field spin resonance spectrometer is shown in Figure 1.

C-1. MARGINAL OSCILLATOR, 150 - 300 MC/SEC

The observed high-field exciton resonance spectrum of $(\phi_3 As CH_3)^+ (TCNQ)_2^-$ indicated that the zero-field transitions would occur at approximately 60 Mc/sec, 160 Mc/sec, and 220 Mc/sec (7). In order to observe the two higher frequency transitions, a coaxial-line marginal oscillator was built, similar in design to that built by La Force (8) for the nuclear resonance of a pure sample of ferromagnetic cobalt.

The oscillator is of the Hartley type (1). Figure 2 is a cross sectional semi-schematic layout of the unit. A more detailed cross sectional diagram showing the mechanical construction is shown in Figure 3.

Several important construction points are outlined below:

a) The coaxial lines in the grid circuit are made from 300 series stainless steel tubing (non-magnetic), of 0.005" wall thickness. The tubing was silver plated to a depth of approximately 0.002". Thin stainless was chosen for two reasons: 1) the sample was to

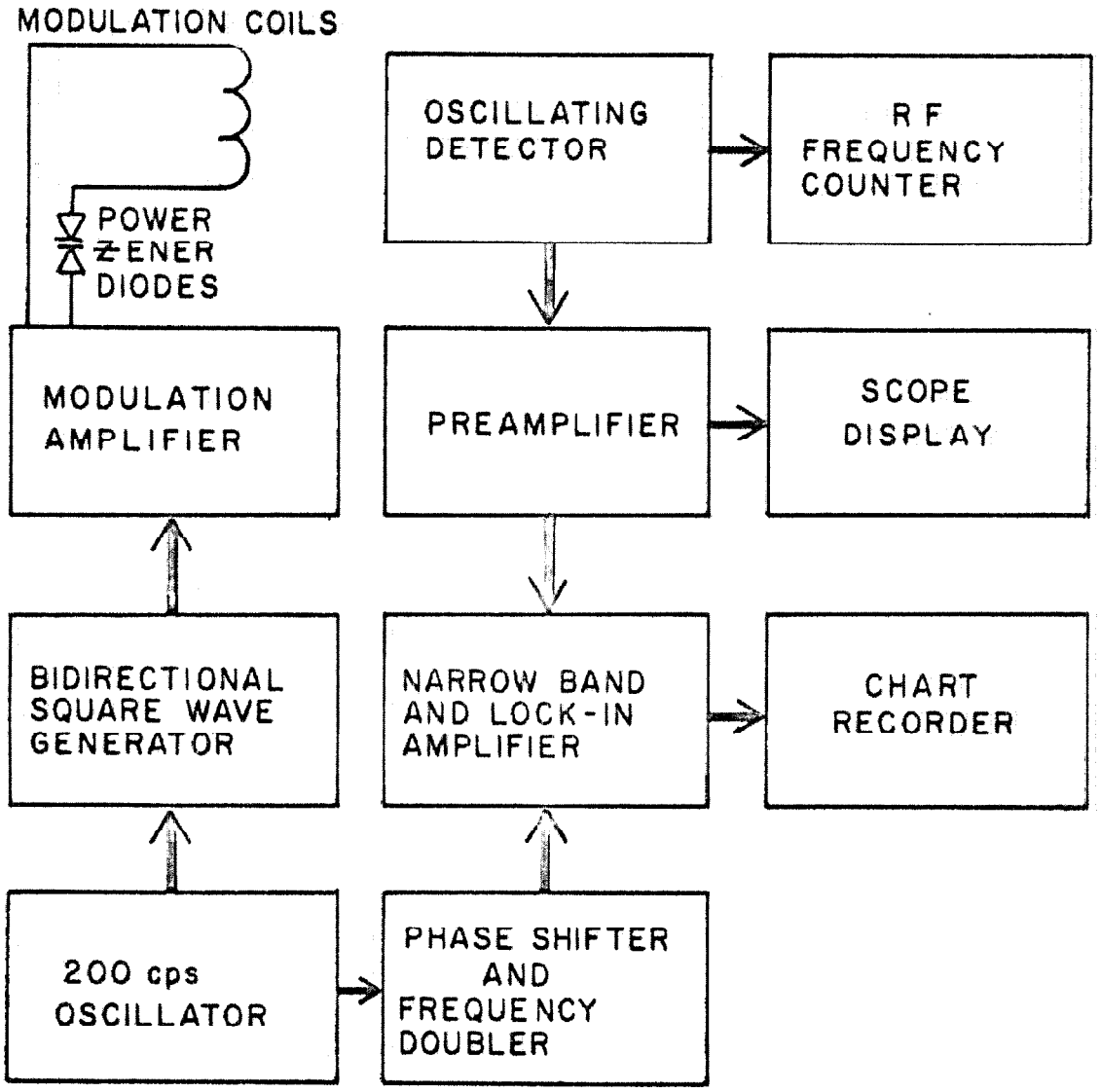

Figure 1. Block Diagram of Zero-Field Resonance Spectrometer.

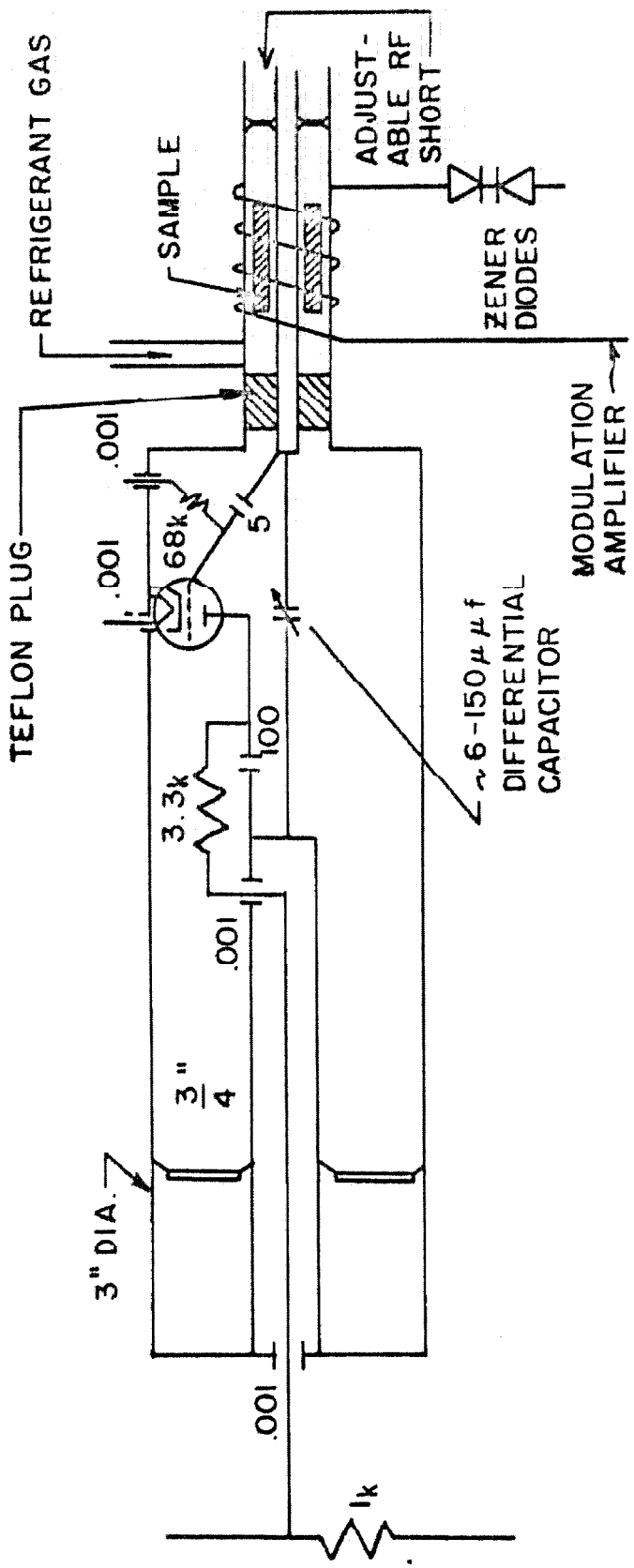

Figure 2. Semi-Schematic Diagram of 150-300 Mc/sec Oscillating Detector.

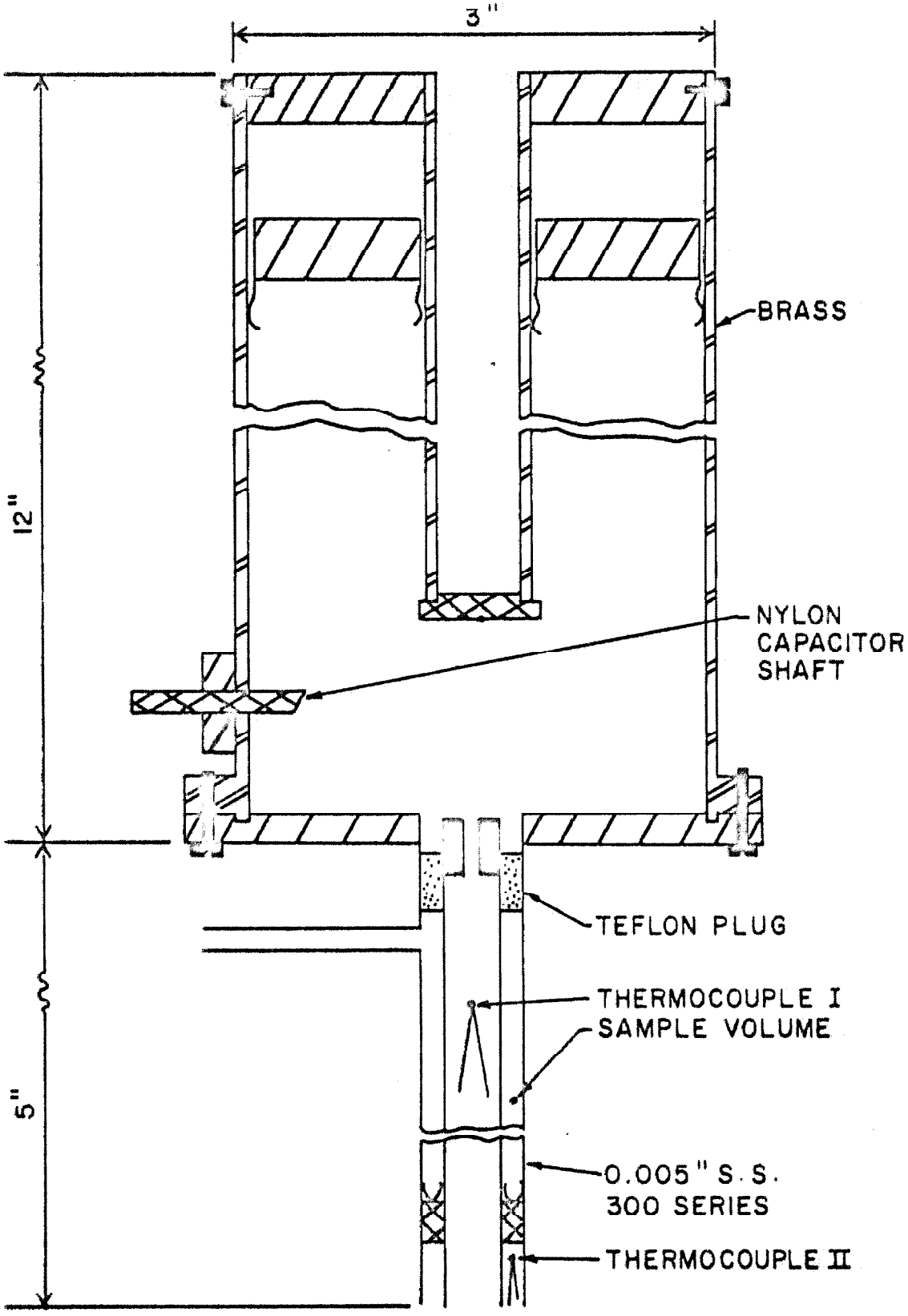

Figure III. Mechanical Construction of Oscillator.

be maintained at a low temperature by cooling the grid line of the oscillator, and thin wall tubing was necessary to cut down on the heat leak to the main part of the oscillator, 2) the modulation system being magnetic field erasure (see page 20), the smallest possible amount of metal within the modulation field was desired, consistent with necessary structural strength.

The approximate inductance of a shorted coaxial line less than 1/8 wavelength long is

$$L = 60 \frac{l}{c} \ln \frac{r_o}{r_i} \quad ,$$

where l is the length, r_o, the radius of the outer conductor, r_i, the radius of the inner conductor, and c is the speed of light.

To vary the inductance, one has the choice of changing either the ratio of the radii of the coaxial lines or their lengths. In order to attain simplicity of construction, as well as to allow gas flow through the grid end, a loosely fitting annular plug was made for both the grid and plate lines. Resilient phosphor bronze fingers were soldered to each plug, providing the mechanical stability necessary to maintain good electrical contact. These annular plugs were moved in order to effect

gross changes in the oscillator frequency. (Commercial finger stock, manufactured by Eitel McCullough, Inc., part number CF 100 X 3, was used in the plate line. The fingers for the grid line were made from a 0.005" phosphor bronze sheet, which was bent and slotted with a 0.007" saw.)

b) The mounting of the tuning capacitor must be as stable as possible. A loose mounting will result in large noise problems. The method we used with a fair degree of success consisted in fixing a nylon shaft to the capacitor with epoxy, and then leading the nylon shaft through an aluminum bearing surface. The aluminum mount was sufficiently long to be beyond electrical cut-off at the frequencies we used. The capacitor, of course, is firmly supported independently of its shaft.

The circuit as constructed by La Force used a butterfly capacitor. Since a small butterfly capacitor with a large variable capacity was commercially unavailable, a differential capacitor was used, of range from about 6 to 150 μμf. Since the circuit is electrically asymmetric with regard to the center plates of the capacitor, a differential capacitor is able to be used satisfactorily (the same would not be true in a push-

pull circuit, where exact balance is critical). In choosing a tuning capacitor, the principal consideration is that there be no sliding electrical contact through which radio frequency current flows.

For this type of coaxial circuit, the placement of the tube, tuning capacitor, and other resistive and capacitive components may be dictated by space considerations rather than by any need to maintain a symmetric, coaxial arrangement of parts.

c) The oscillator level control circuit is shown schematically in Figure 4. Modifications of the published circuit (8) were made after discussion with Dr. La Force. The major change is the elimination of the voltage regulator tube (an OB-2 type), because of general instability under varying load conditions.

The oscillator stays in operation with grid currents ranging from about 5 to 50 microamperes. With the grid current above approximately 25 microamperes, however, the level of oscillation is more determined by the characteristics of the vacuum tube, and less affected by the small change in loading caused by resonance absorption by the sample. In normal operation, grid

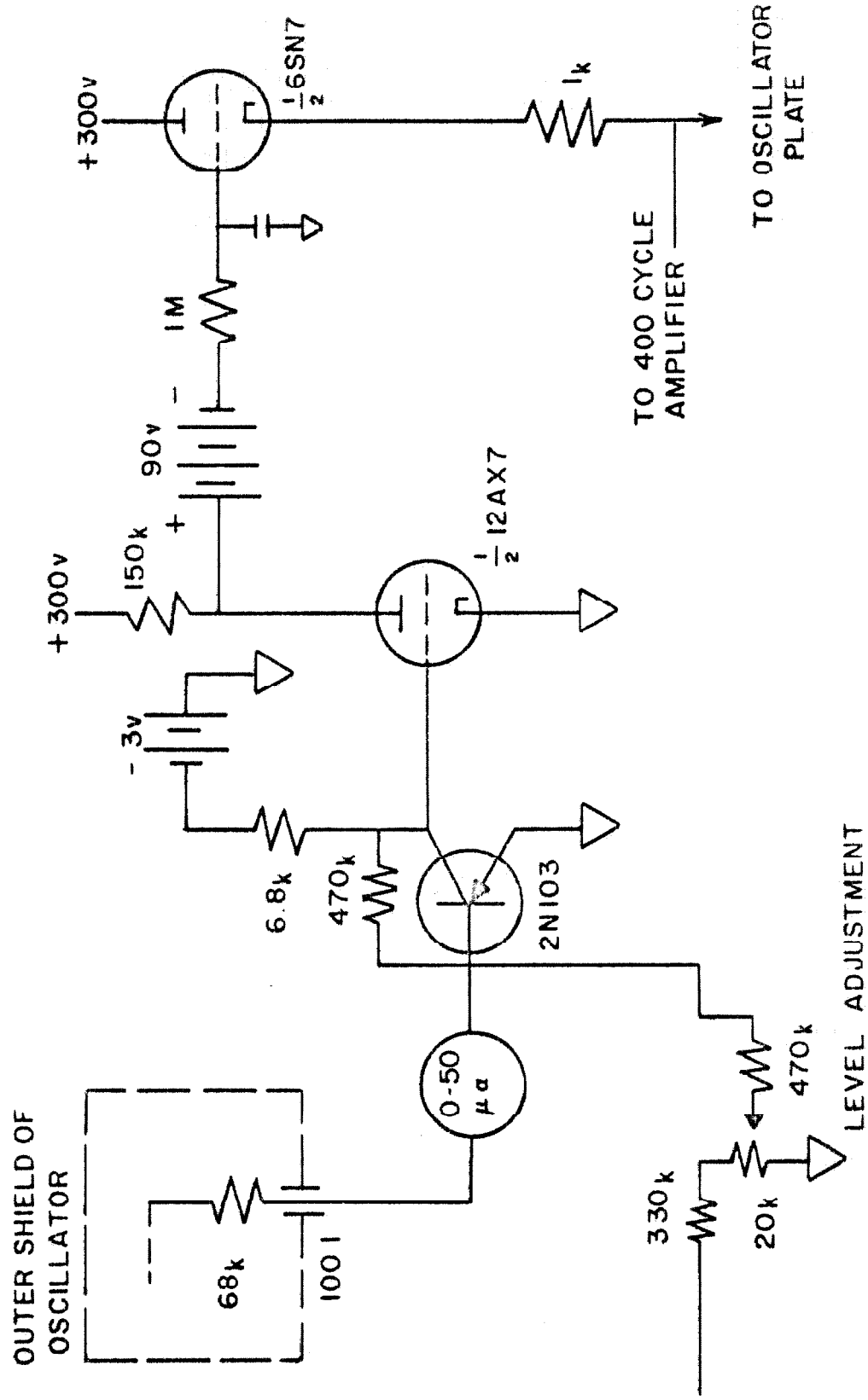

Figure 4. Oscillator Level Control Circuit.

currents ranging from 8 to 12 microamperes were used.

In addition to monitoring the grid current, the plate voltage was intermittently checked. To eliminate microphonics from the meters, bypass switches were provided. Generally, however, the major sources of microphonics will be mechanically loose parts, and the oscillator tube itself.

d) In order to measure the frequency, the output of a small loop placed in the plate line of the oscillator, was fed to a Hewlett Packard Model 540B Transfer Oscillator. As the marginal oscillator would scan frequency, it would zero beat with known frequency settings of the transfer oscillator. The transfer oscillator frequency was set using a Hewlett Packard Model 524C Frequency Counter.

The principal problem in using the transfer oscillator results from the coupling of the radio frequency power of the transfer oscillator into the coaxial line. The zero beat of the two oscillators that occurs in the coaxial line causes a very large amplitude modulation of the marginal oscillator. Two ways to minimize this effect are: 1) use of a buffer stage, e.g., a wide band amplifier

between the two oscillators, and 2) use of harmonics to measure the fundamental frequency whenever possible.

e) A gas-flow cooling system was used in order to vary the sample temperature. For thermal insulation, the sample-containing end of the coaxial oscillator was encased in styrofoam, which was 1/2" thick and extended about one inch past the end of the oscillator. The coolant gas was directed back over the 120 turn solenoidal modulation coil, which was wrapped around the styrofoam. (See Fig. 5). To provide greater heat capacity, and to eliminate thermal gradients across the sample, a copper tube, slit lengthwise, was placed around the stainless grid line. The copper was electrically insulated from the grid line with adhesive* tape, but good thermal contact between the two was attained by bonding them together with General Electric No. 7031 Adhesive Insulating Varnish diluted with toluene (9). The sample temperature was measured with two thermocouples, one in the center of the grid coaxial line, the other in the annular region immediately after the radio frequency short (See Fig. 3). Temperature differences in thermo-

*Cloth base adhesive tape has been found satisfactory at temperatures down to 4° K, providing a good bond has been made at room temperature. Temperature cycling causes almost no deterioration.

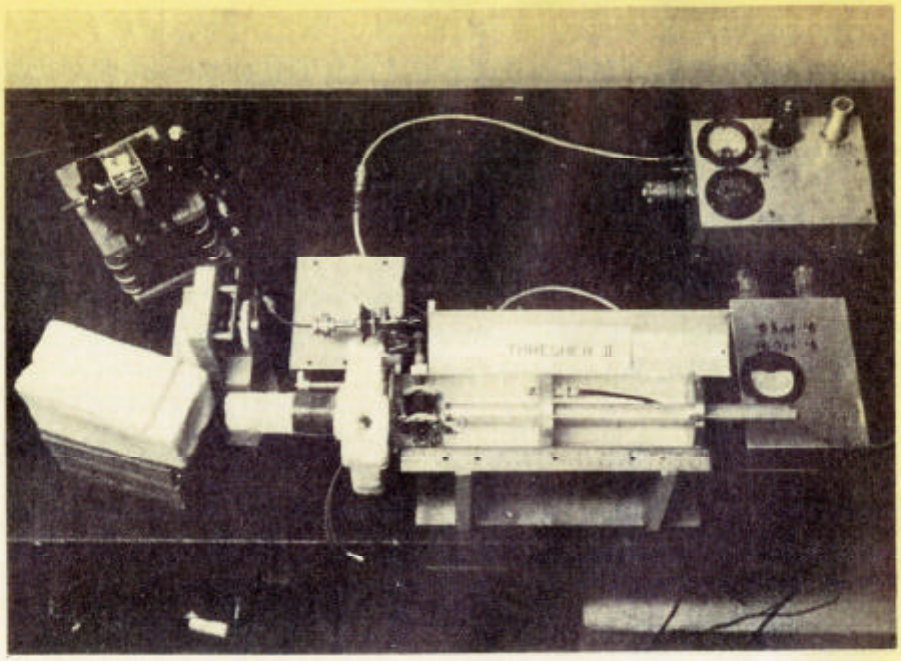

Figure 5a. View of Open Oscillator.

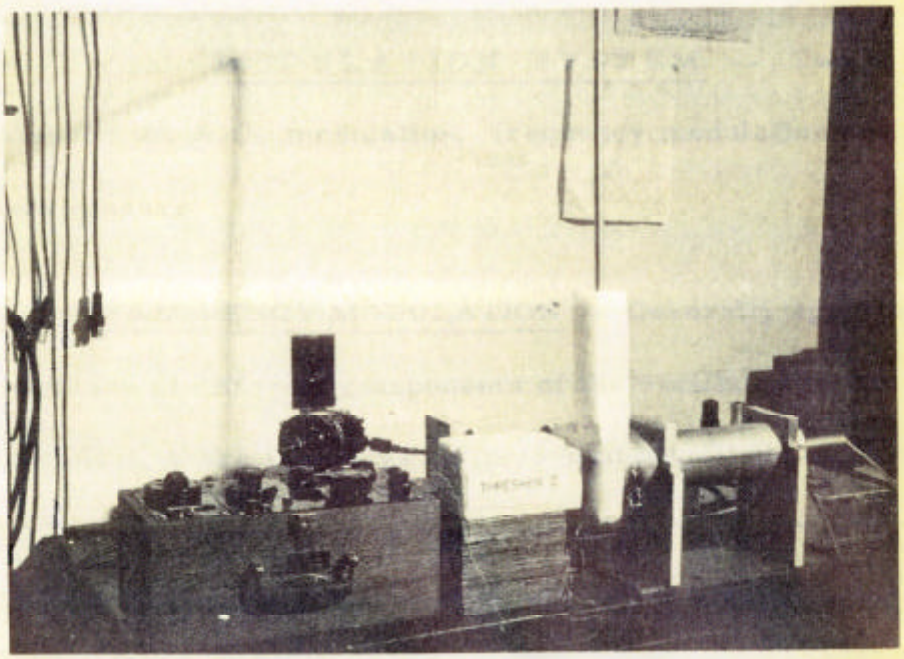

Figure 5b. Oscillator with Transfer Tube.

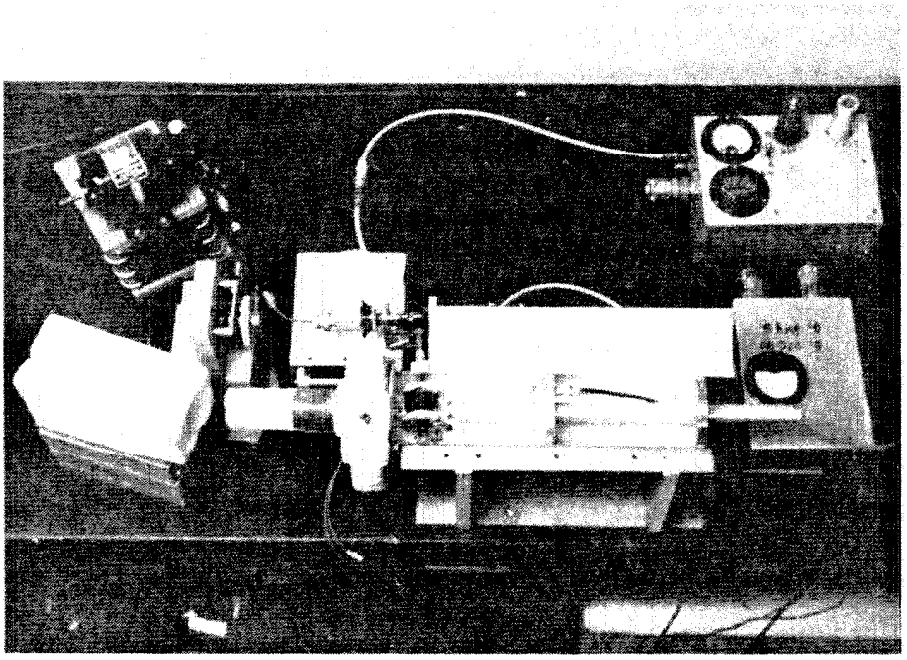

Figure 5a. View of Open Oscillator.

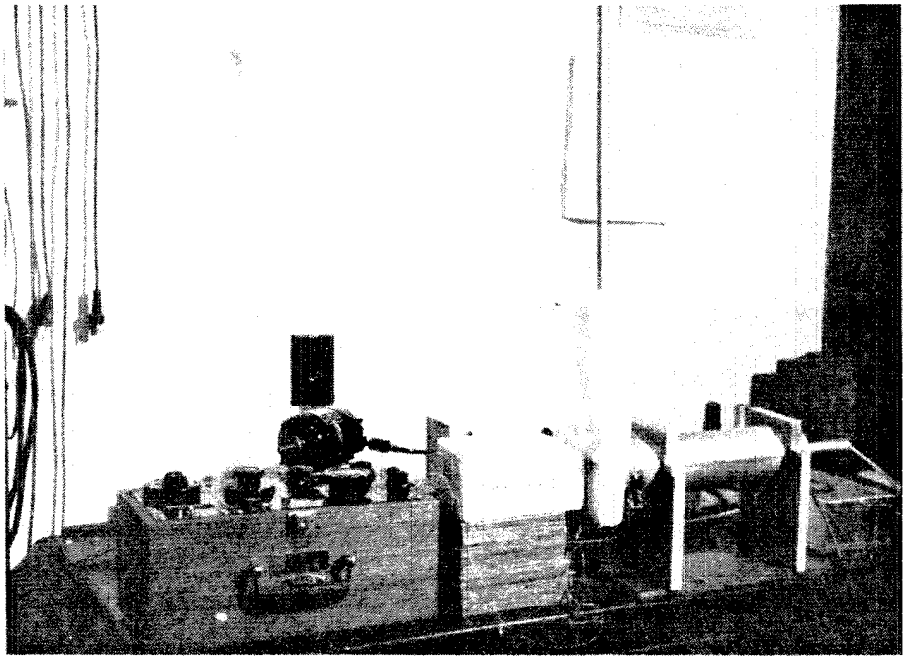

Figure 5b. Oscillator with Transfer Tube.

couple readings were generally less than $1/2^{\circ}$K.

The refrigerant gases, nitrogen and helium, were obtained at a constant flow rate by boiling their liquids with resistance heaters. This method proved far more stable than any method which involved pressurizing the dewars with room temperature gas. The tip of the transfer tube was kept above the liquid level. A residual pressure of CO_2 gas was used in the transfer tube, so that there would not be a sharp change in heat loss properties in the range around the condensation temperatures of oxygen and nitrogen, which was the temperature range most used.

C-2. MODULATION SYSTEM -- Two possibilities exist for the A.C. modulation: frequency modulation and magnetic field erasure.

FREQUENCY MODULATION -- Generally speaking, since the reactance of different components of the oscillator is frequency-dependent, there is always an incidental amplitude modulation of the radio frequency power when an oscillator is frequency modulated. This incidental amplitude modulation is, of course, coherent with the reference voltage of the lock-in detector, and can pass through the narrow-band detection system unattenuated. When the magnitude of

the incidental amplitude modulation is independent of the oscillator frequency (approximately true in our case), the amplitude modulation can be bucked out by introducing, at the first stage of amplification, a coherent signal of opposite phase. This is generally necessary since the incidental modulation is very often large compared to the amplitude modulation caused by resonance absorption, and early stages of amplification will saturate.

Initial experiments, in tuning up the oscillator, were done using frequency modulation to observe the Co^{59} nuclear magnetic resonance in ferromagnetic cobalt (8). Frequency modulation, however, is most useful in nuclear quadrupole resonance work, where the lines are only a few kilocycles wide. Our exciton resonances, however, were expected to be of the order of megacycles wide, and it would have been almost impossible to have swept through the whole resonance absorption line with one modulation cycle. A smaller sweep would result in a proportionate reduction in signal. With the smaller sweep, derivative curves would be obtained, which would have been distorted if the frequency modulation were not small compared to the line width. This reduction in signal-to-noise ratio, and the possible ambiguities in line shape, led us to abandon frequency modulation for the exciton work. All of the exciton spectra were obtained using magnetic field erasure, as described in the next section. At present, however, in spite of the above considerations, I believe

that it would be worthwhile to design a system using frequency modulation to detect the exciton signals. Certain difficulties were encountered in completely erasing the line using magnetic field modulation. This was especially true of the broader lines, at the higher temperatures. The signal to noise of the higher temperature lines is great enough so that the reduction of signal intensity should not be too troublesome.

MAGNETIC FIELD ERASURE -- By applying a moderately large magnetic field (50 gauss) to the sample, the resonance is broadened and its frequency is shifted. A pulsed magnetic field, therefore, will alternately turn the resonance absorption signal on and off. However, since the size of most spectrometers is relatively small (to keep inductive effects of leads to a minimum, etc.), the major problem in pulsing the magnetic field is the pick-up of the pulsed field in the various oscillator components.

A convenient way to minimize the effect of pick-up is the use of a bidirectional square wave for the magnetic field modulation (10)(2). As can be seen in Figure 6, the fundamental of the pick-up occurs at f_p, which is one-half the frequency of the absorption signal f_s. The pick-up is rejected by the narrow-band detection system. Here also we must make sure that the early stages of amplification are not saturated. The pick-up signal can be bucked out as previously described, if necessary.

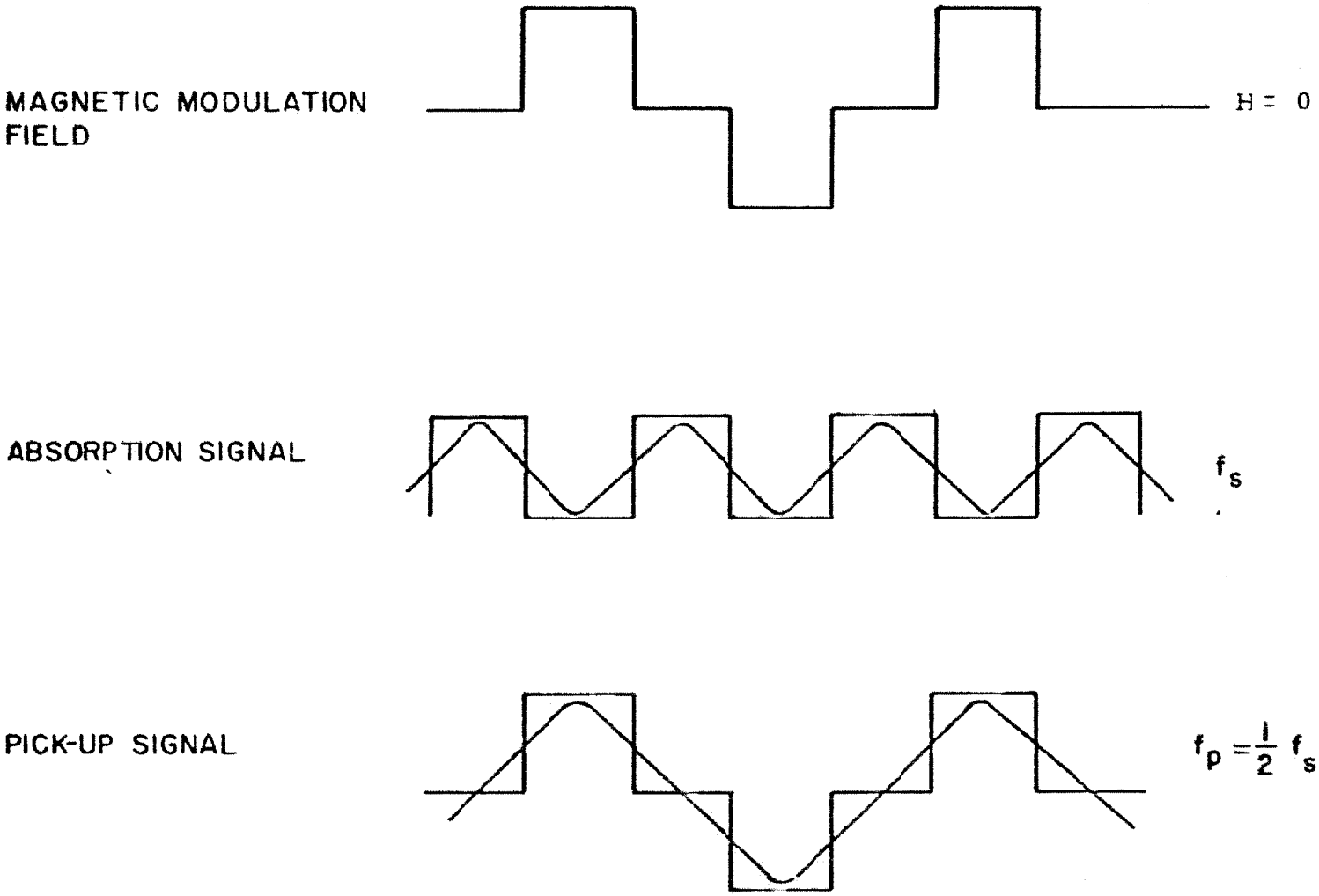

Figure 6. Zeeman on-off Modulation Waveform; Absorption and Pick-up Signals.

Two different circuits were used to obtain the Zeeman on-off modulation. The first (See Fig. 7) is easy to build, quite inexpensive, and gives an output that is relatively steep. Both the height and the width of each pulse are variable. The circuit basically uses the clipping characteristics of Zener diodes to take a very small segment of a large amplitude sine wave, during the positive and negative parts of each cycle. This approximates a bidirectional square wave fairly well. Alternatively, in later experiments, a Tektronix Type 162 Waveform Generator, used with two Tektronix Type 161 Pulse Generators, can provide the bidirectional waveform. The output from this circuit is quite square, compared with the somewhat rounded output of the Zener circuit. The cost is relatively high, and the limiting waveform, it turns out, is not determined in this step.

In both cases the bidirectional square wave signal is then used to drive a 70 watt Heathkit audio amplifier. In order to make sure that no current would flow during the off-time, the output of the amplifier was further clipped by two 6 volt power Zener diodes. In our experiments the detection frequency was 400 cps.

The amplifier was used to drive the modulation coil, and it was in this step that the shape of the waveform was limited by the inductance of the coil. Even if power amplifiers had perfect fidelity (infinite bandpass), there is a fundamental limitation on the rise time and, thus, upon the shape of the modulation field. The total work

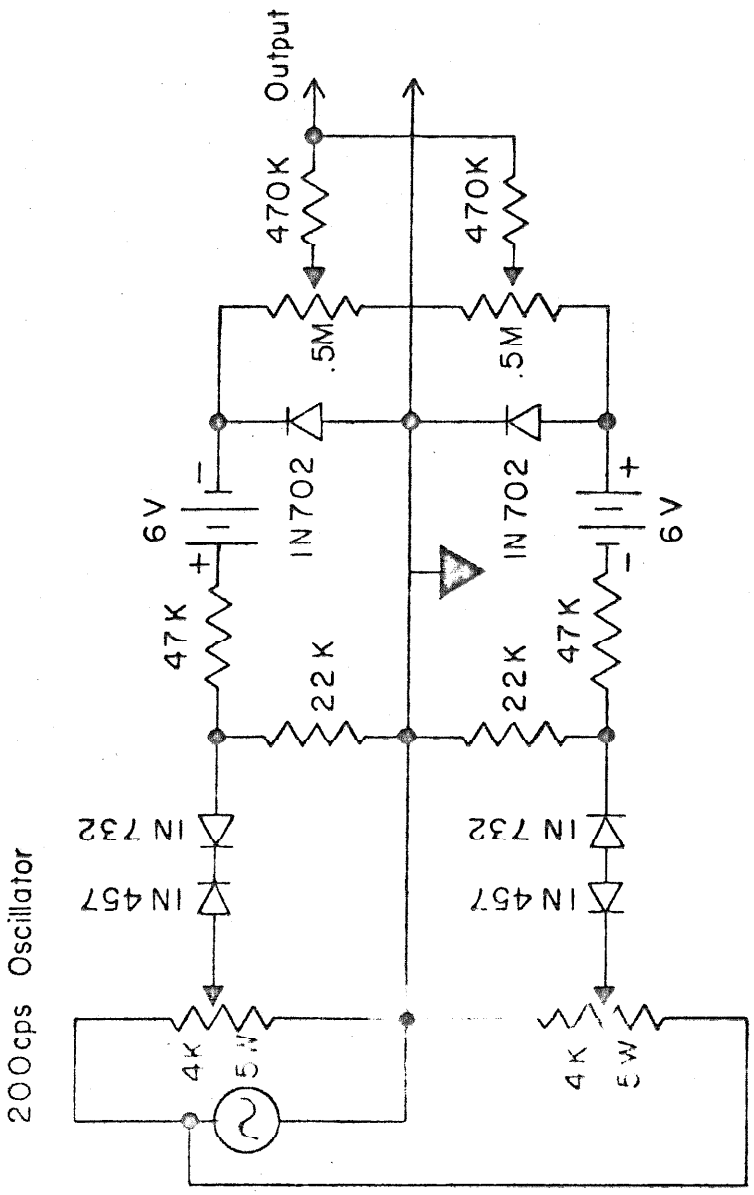

Figure 7. Bidirectional Waveform Generator.

required to build up a current I in a circuit of inductance L is

$$T = 1/2\ LI^2 .$$

The power required to do this work in time τ is

$$P = T/\tau = 1/2\ LI^2/\tau .$$

In practice this meant that our amplifier output was averaging between 2 and 8 watts average power. With levels higher than this, there was a noticeable distortion of the waveform, even though the amplifier had much higher average power capabilities.

C-3. DETECTION SYSTEM -- Because of non-linear characteristics of the oscillator tube, the amplitude modulation of the oscillator, caused by spin resonance absorption, can be detected directly on the D.C. plate lead. Alternately, a loop could have been placed in the oscillator, and the sampled radio frequency power detected with a crystal detector. The 400 cps signal was amplified with a low noise preamplifier* (Fig. 8), and fed through a Packard and Burns Model #60 narrow-band amplifier. The amplified signal was then phase-sensitive detected and displayed with a Brown Potentiometer Chart Recorder.

Figure 9a is a dual trace oscillograph of the i) absorption signal before narrow-band amplification and ii) the current waveform of the bidirectional modulation. Figure 9b shows the same absorption signal after the narrow-band amplifier.

* Circuit suggested by A. Hildebrandt, of this laboratory.

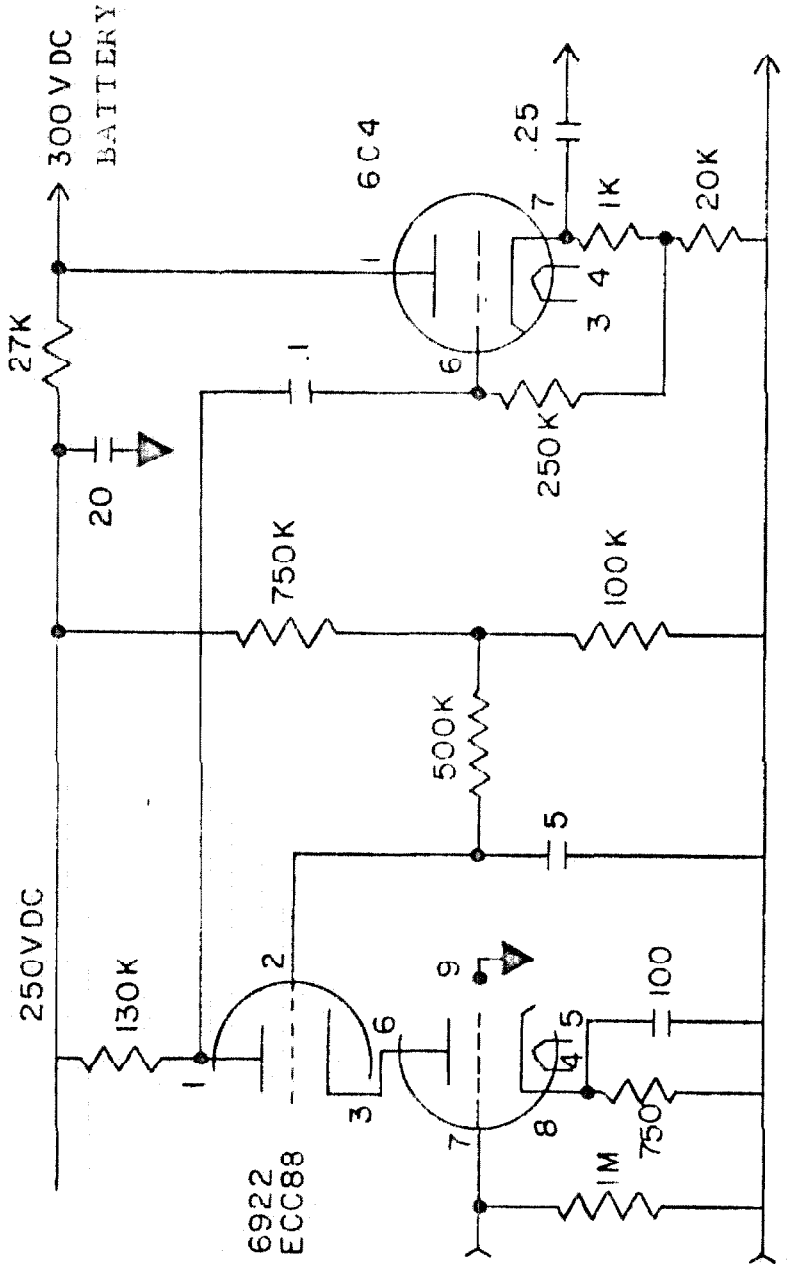

Figure 8. Low Noise Preamplifier

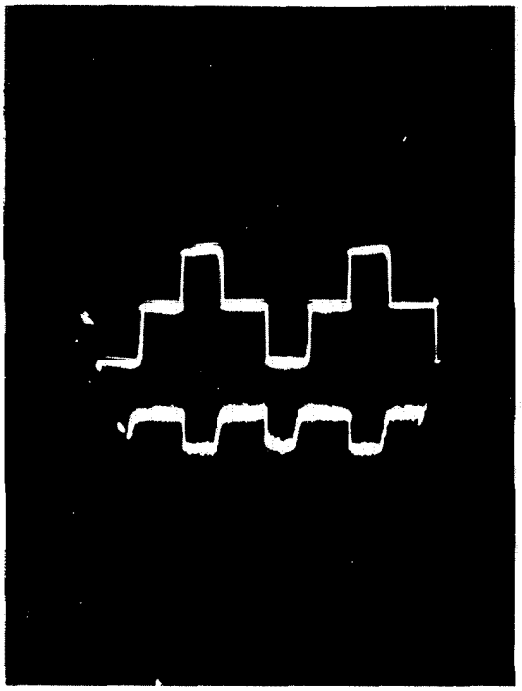

Figure 9a.

1. Bidirectional Zeeman Modulation Field.

2. Absorption Signal before Narrow-band Amplifier.

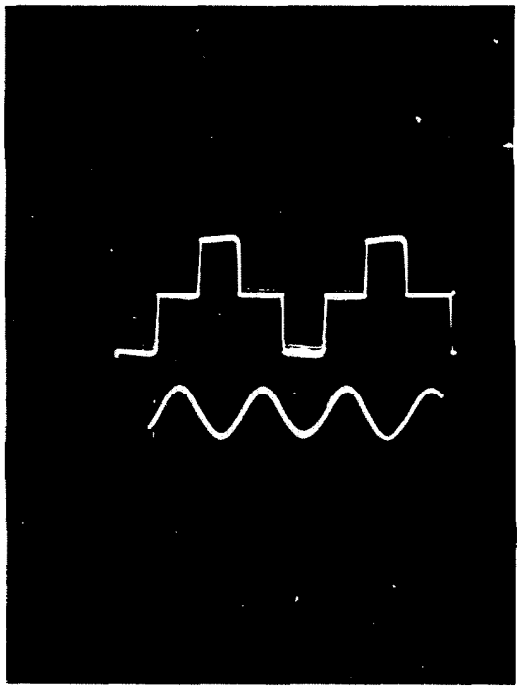

Figure 9b.

1. Bidirectional Zeeman Modulation Field.

2. Absorption Signal after Narrow-band Amplifier.

Figure 10 is a circuit diagram of the lock-in detector that was used. Figure 11 shows the 200 cps→400 cps frequency doubler, and Figure 12 shows the phase shifter used to compensate for possible phase changes introduced in the amplification of the resonance signal. These three pieces of equipment were built in our laboratory by Mr. Donal D. Thomas, and used with his permission. It should be noted that there is no need for a frequency doubler when using the Tektronix Waveform Generator to obtain the modulation waveform, the required circuitry being self-contained.

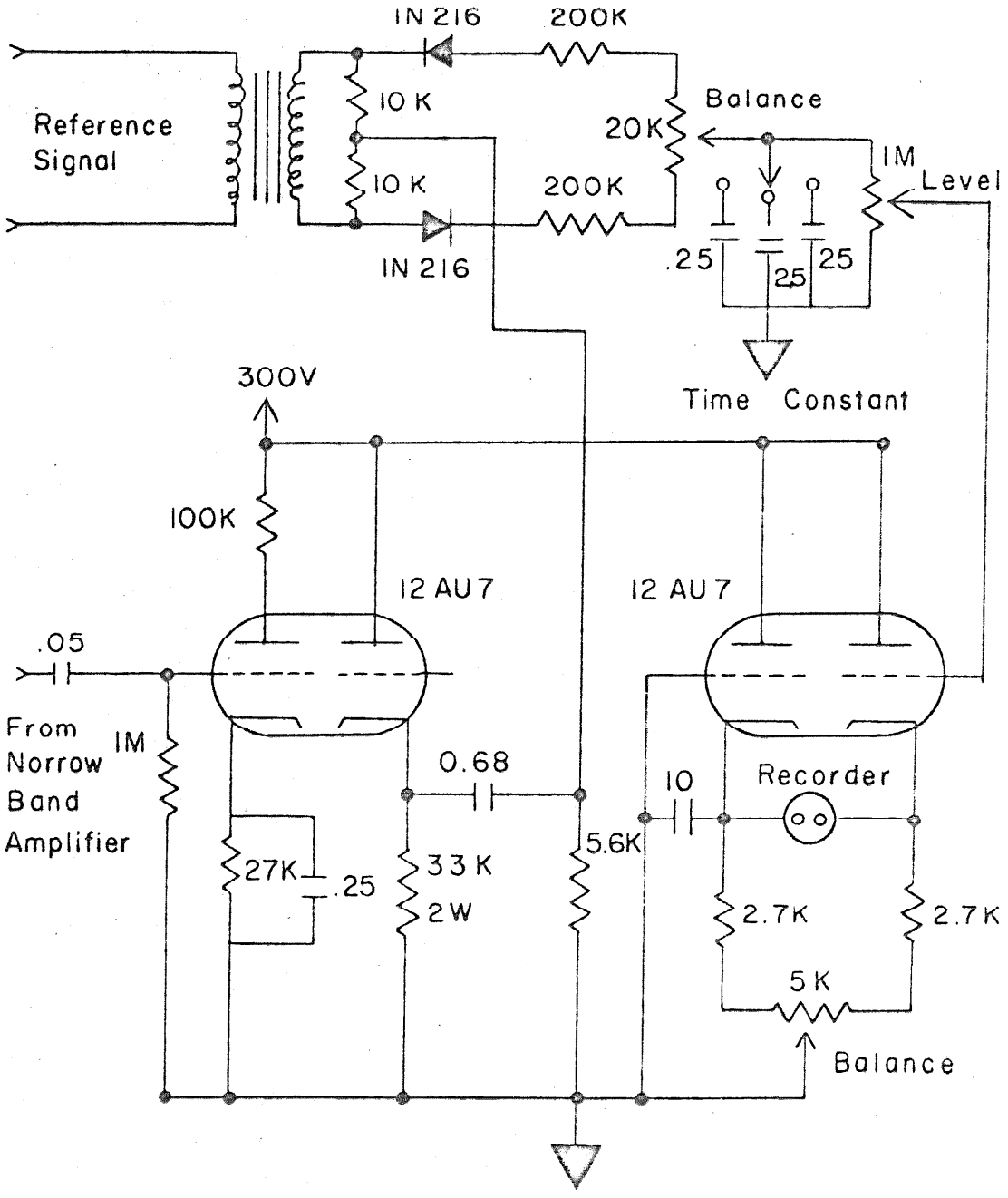

Figure 10. Lock-in Amplifier.

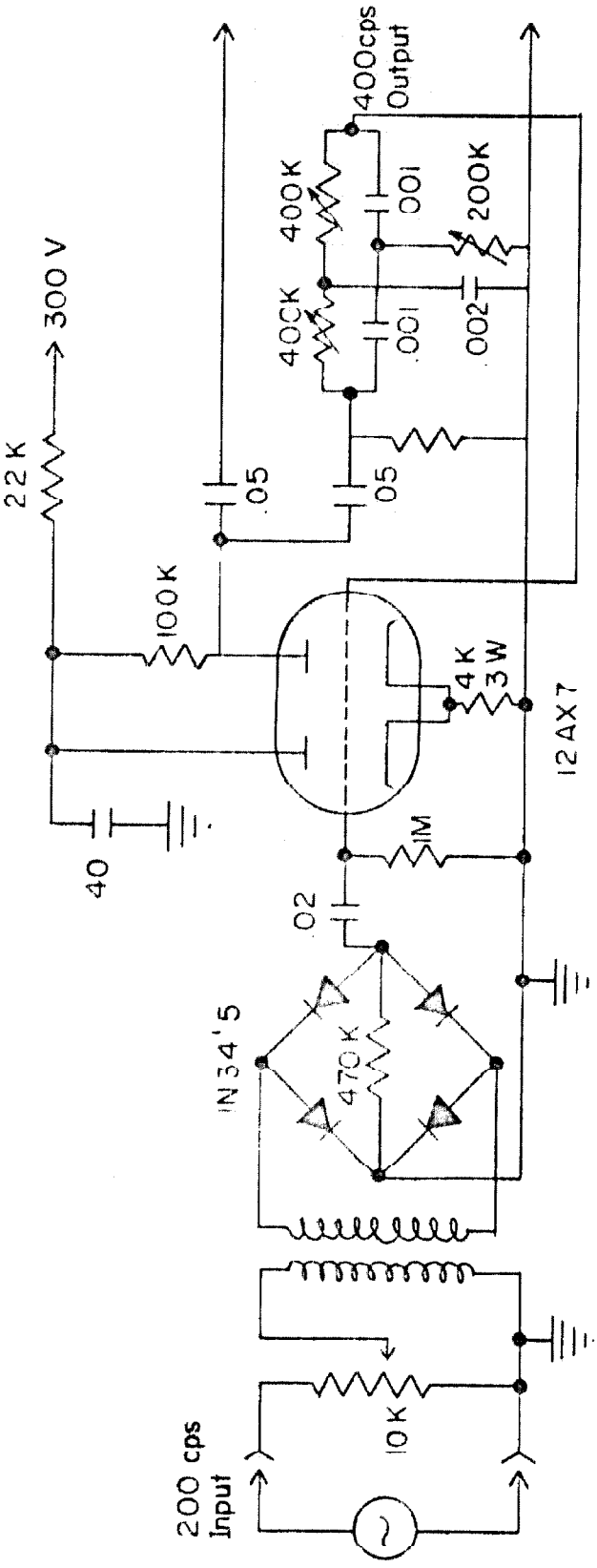

Figure 11. Frequency Doubler.

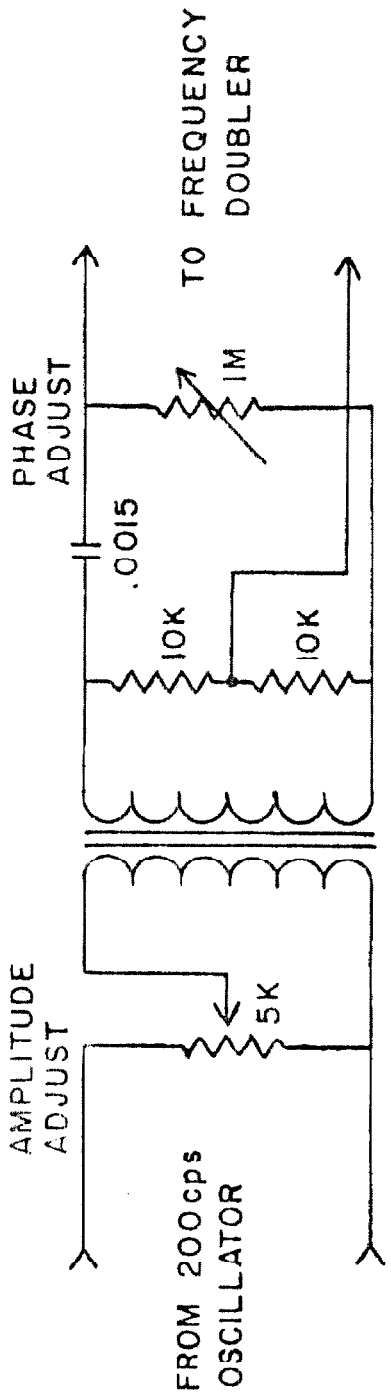

Figure 12. Phase Shifter.

PART II

TRIPLET EXCITON SPIN RESONANCE IN ZERO FIELD

A. INTRODUCTION

Professor H. M. McConnell, et al., have suggested that below a certain transition temperature (previously considered to be a paramagnetic → antiferromagnetic transition temperature), many solid free radicals become diamagnetic, and that in this state the elementary electronic excitations are paramagnetic triplet excitons (11, 12).

The idea of an exciton as an atomic or molecular excitation capable of propagating through a linear, perfect lattice had been introduced by Frenkel (13) in 1931 and applied to the study of optical spectra of crystals. Important contributions to the theory of singlet excitons have been made by Davydov (14). The following discussion of triplet excitons is based upon the above-cited works of McConnell.

Aromatic molecules are relatively large and unsymmetrical crystal-structure units, resulting frequently in crystal structures in which any given molecule reacts most strongly with one (Class I) or perhaps two other molecules (Class II crystal). When the individual molecules in Class I crystals are spin 1/2 free radicals, spin exchange within pairs of molecules leads to a singlet ground state and an excited triplet state for each pair. The translational symmetry of the lattice implies the equivalence of all unit cells, and the excitation can propagate through a lattice of unexcited pairs as a triplet exciton.

For Class II crystals the spin of any radical interacts equally with two other spins, giving rise to linear chains which are unstable with regard to distortions that produce an alternation of the distances between interacting units. The chains are, therefore, energetically unstable with respect to a transition to a Class I crystal -- if the exchange interaction is greater than the thermal energies. Since the formation of one singlet pair increases the probability of formation of neighboring singlet pairs and increases the exchange interaction within the pairs, a sharp decrease in the paramagnetic susceptibility is expected as soon as $kT < J$ (exchange interaction energy). Experimental studies of thermally excited triplet systems give strong support to the above predictions (15, 16, 17, 18, 19).

The present work reports the study of the charge transfer solid free-radical complex of $(\phi_3 As CH_3)^+ (TCNQ)_2^-$ in zero magnetic field. The spin-resonance properties are consistent with a Class I crystal throughout the temperature range investigated. The above-cited experimental work on Wurster's Blue Perchlorate(19) shows that it is a Class II crystal which undergoes a transition to a Class I crystal(coinciding with an orthorhombic $\longrightarrow$ monoclinic phase transition).

B. ZERO-FIELD SPIN HAMILTONIAN

In the absence of an external magnetic field, the spin-spin dipolar Hamiltonian, $\mathcal{H}$, for a linear triplet exciton system has the form:

$$\mathcal{H} = g^2\beta^2 \sum_{j>i} (\vec{S}_i \cdot \vec{S}_j) r_{ij}^{-3} - 3 (\vec{r}_{ij} \cdot \vec{S}_i)(\vec{r}_{ij} \cdot \vec{S}_j) r_{ij}^{-5}, \quad (1)$$

where $\vec{r}_{ij}$ is the position vector connecting electrons i and j,

and $\vec{S}_i$ is the spin angular momentum operator for electron i in units of $\hbar$.

Choosing an appropriate axis system, equation (1) can be reduced to the familiar $\underline{D}$ and $\underline{E}$ Hamiltonian:

$$\mathcal{H} = D S_z^2 + E (S_x^2 - S_y^2) \quad (20). \quad (2)$$

Whether one considers an exciton to be either a distributed excitation or a fairly localized excitation moving or diffusing rapidly through the crystal, the nuclear hyperfine structure should be averaged out, and, therefore, these terms are neglected in the Hamiltonian.

The following trivial change in notation will prove useful in later discussions:

$$\mathcal{H} = X S_x^2 + Y S_y^2 + Z S_z^2 . \quad (3)$$

EIGENFUNCTIONS, EIGENENERGIES, AND TRANSITION PROBABILITIES

Using equation (2) we obtain the following eigenfunctions:

$$|x\rangle = \frac{|1\rangle + |-1\rangle}{\sqrt{2}} = \frac{\alpha\alpha + \beta\beta}{\sqrt{2}} \qquad (4a)$$

$$|y\rangle = \frac{|1\rangle - |-1\rangle}{\sqrt{2}} = \frac{\alpha\alpha - \beta\beta}{\sqrt{2}} \qquad (4b)$$

$$|z\rangle = \frac{|0\rangle}{1} = \frac{\alpha\beta + \beta\alpha}{\sqrt{2}} \qquad (4c)$$

From equations (2, 3, 4) we obtain the energies:

$$E_x = D + E = Y + Z \ ,$$

$$E_y = D - E = X + Z \ , \quad \text{and}$$

$$E_z = 0 = X + Y \ .$$

The relative transition probabilities for spin resonance absorption are given by the square of the spin matrix elements,

$$P_{i \to j} \propto |\langle i|S_k|j\rangle|^2 \ (k, i, j = x, y, z) \ . \qquad (5)$$

From equation (4) we obtain three zero-field transitions of equal probability, with frequencies of $Y - Z\ (\nu_x)$, $X - Y\ (\nu_z)$, and $X - Z\ (\nu_y)$. In future discussion, we shall assume that ν_x is x-polarized, i.e., the radio frequency power being absorbed is polarized in the x direction. Figure 13 shows the energy levels, transition frequencies, and assumed direction of polarization of the transition.*

---

* For the axis system x, y, z defined above, one can be certain that the highest frequency transition is y-polarized, but the polarizations of the two lower frequency transitions are not determined by the relative magnitude of the transition frequencies.

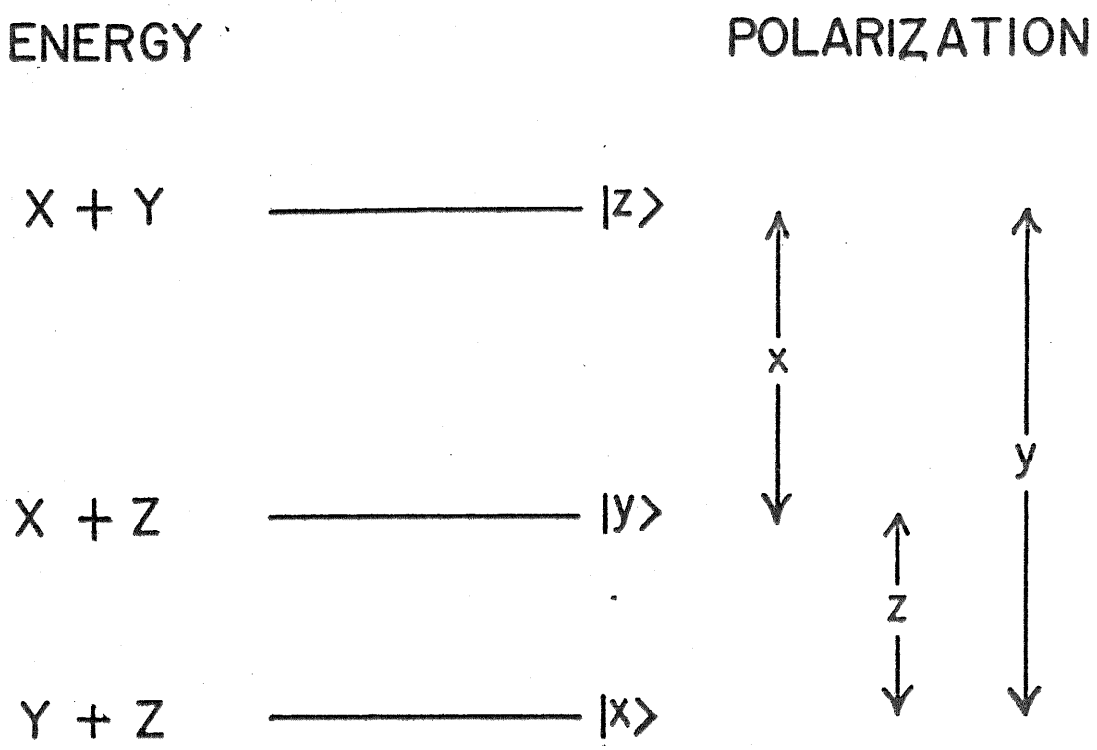

Figure 13. Zero-field Energy States

The Spin Hamiltonian is

$$\mathcal{H} = X S_x^2 + Y S_y^2 + Z S_z^2 .$$

The high-field (3000 gauss) splittings in $(\phi_3 As CH_3)^+(TCNQ)_2^-$, observed by Chesnut, et al., correspond to transition frequencies (15) 215.4 Mc/sec (y-polarized), 156 Mc/sec (x-polarized), and 58.8 Mc/sec (z-polarized).

C. EXPERIMENTAL RESULTS

Observed resonance spectra are given in Figures 14, 15, 16 and 17. The transition occurring at 61 Mc/sec in Figure 14 was observed in this laboratory by D. D. Thomas.

The spectra in Figures 14 and 15 were taken using a polycrystalline sample kindly given us by Dr. D. Chesnut of E. I. du Pont and Company. This sample contained a concentration of a spin 1/2 free-radical impurity of approximately 0.01%. The spectra shown in Figure 16, and the upper spectrum of Figure 17, were taken using a sample prepared in this laboratory. In this second sample the spin 1/2 free-radical impurity concentration was about 1.0%. The TCNQ for the second sample was synthesized by Dr. Heimo Keller.

Figure 14 shows the three zero-field resonance absorption curves at 111°K. Note that the line shapes of the three curves are Lorentzian, and have the same width to within experimental error. The line widths were measured at three-quarters height, which corresponds to the points of maximum slope. This was done for easy comparison with high-field data, where derivative curves are usually obtained, and peak-to-peak line widths reported. The principal uncertainty in the line widths of the two higher frequency transitions results from difficulty in estimating the base line. By successively approximating the base line, and plotting calculated points on the spectra, this problem was resolved. Such a problem does not exist with

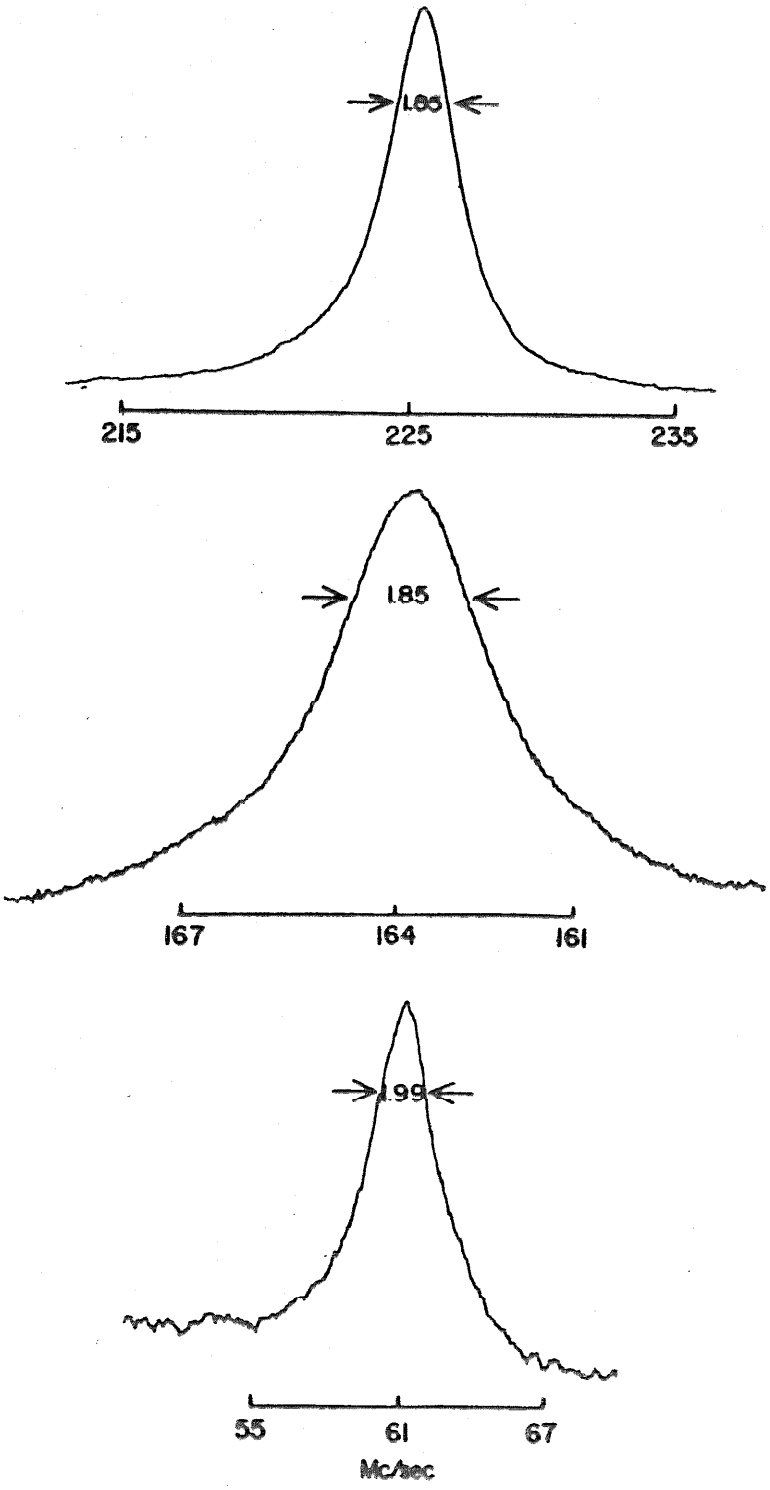

Figure 14. Zero field exciton magnetic resonance signals in $(P_3 As CH_3)^+(TCNQ)_2^-$ at 111 °K. Line Widths are measured at points of maximum slope.

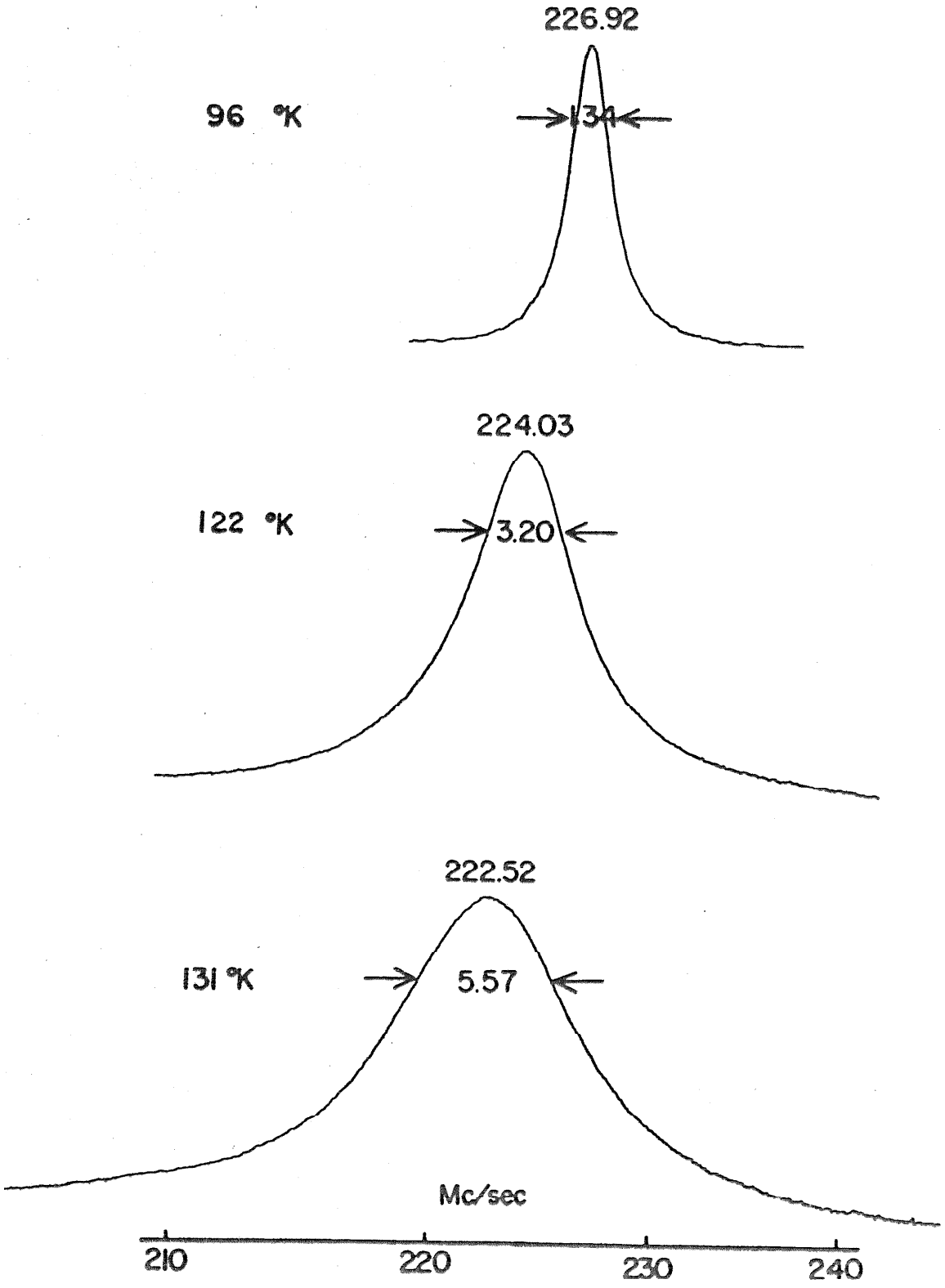

Figure 15.

The y-polarized transitions in $(\emptyset_3 AsCH_3)^+ TCNO)_2^-$ at 96°K, 122°K, and 131 °K.

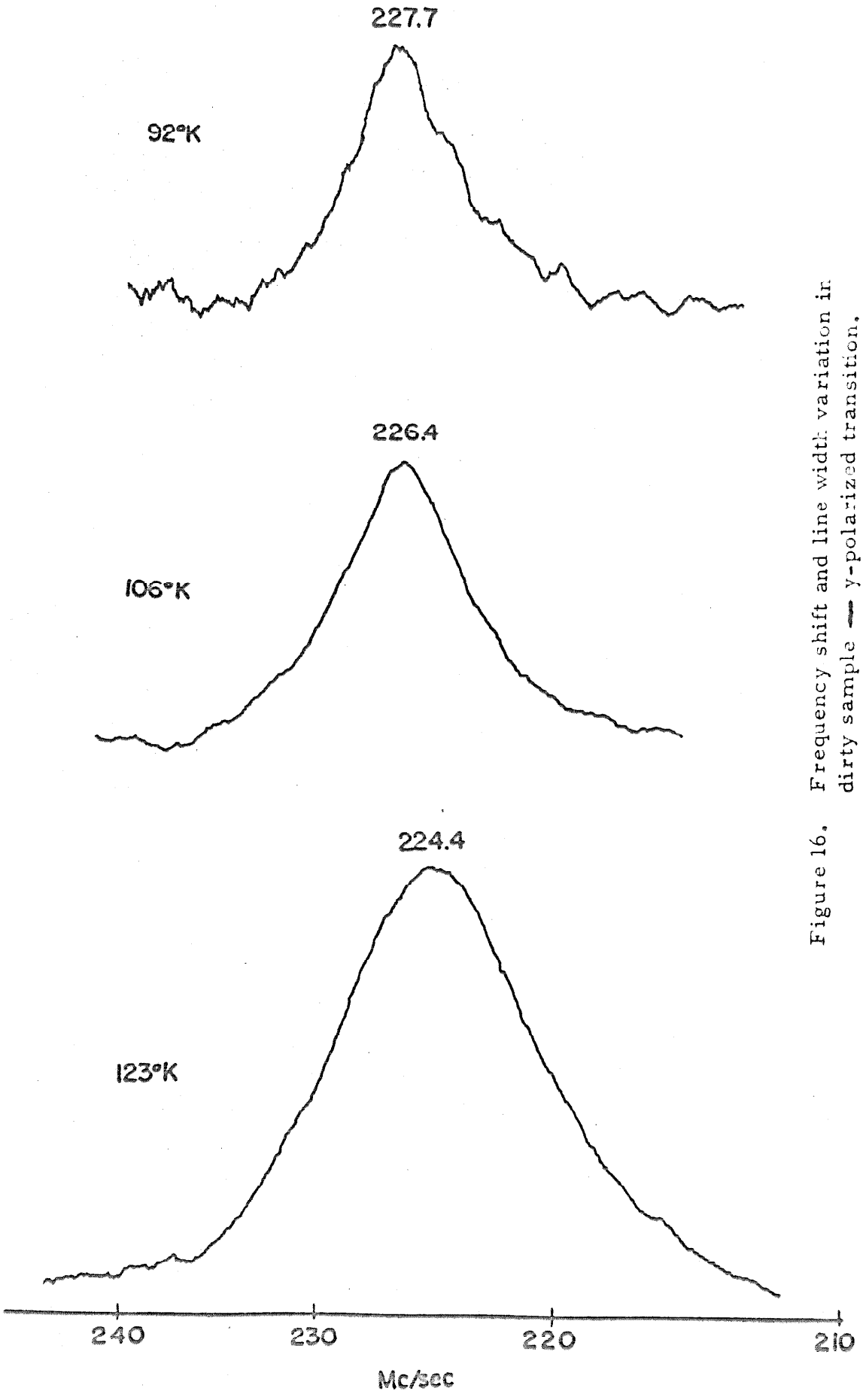

Figure 16. Frequency shift and line width variation in dirty sample — y-polarized transition.

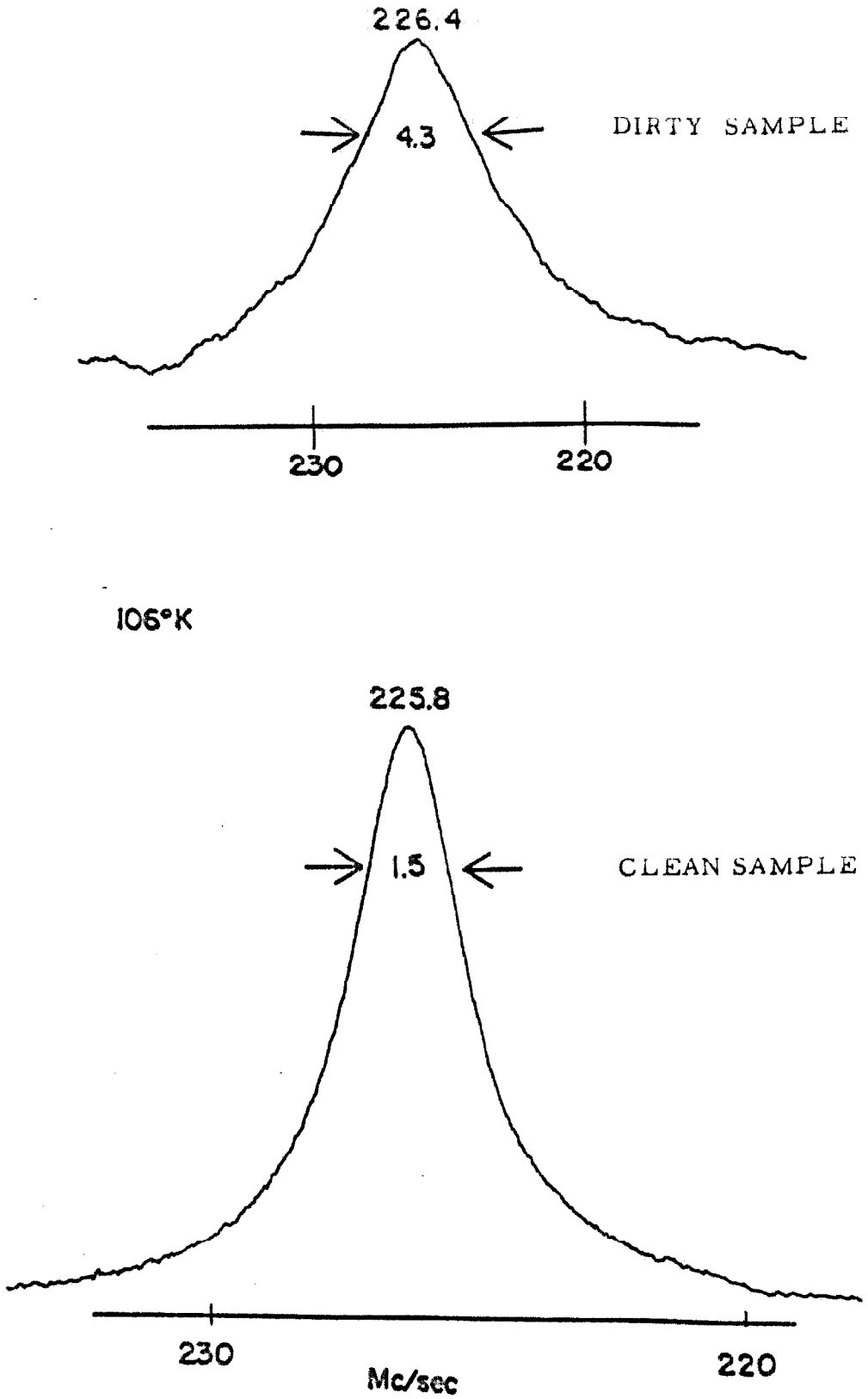

Figure 17. Comparison Spectra of Clean and Dirty Sample - Taken at Same Temperature

derivative curves, where the maxima and minima are well defined.

Figure 15 shows the temperature dependence of the line width and frequency for the y-transition. At higher temperatures there is a substantial shift of the resonance frequency to lower values, as well as substantial line broadening. The x and z transitions show similar shifts and broadenings. At all temperatures studied, the line widths for the three transitions were the same at a given temperature, and the resonance curves, although substantially broadened, retained a symmetrical, Lorentzian line shape. The apparent asymmetry, shown especially in the broadest line in Figure 15, is due to a non-linear scan rate, which makes the line appear to drop faster at the higher frequency end.

Figure 16 shows the temperature dependence of the line width and frequency for the y-transition in the "dirty" sample. A comparison of the clean and dirty samples can be seen in Figure 17, where two spectra taken at the same temperature are shown. Similar line broadening was observed in the x-polarized transition (160 Mc/sec), but the frequency shift was in the other direction. This would indicate an even greater shift for the lowest frequency transition, both percentage wise and in absolute magnitude. This was not experimentally verified.

The temperature dependence of the x and y transitions is

graphically shown in Figure 18. The solid curves refer to the sample supplied by du Pont, the clean sample; the dotted curves pertain to the dirty sample. To within experimental error, the frequency of the z-transition, observed by D. D. Thomas, was found to be equal to the difference of the two higher frequency transitions. A theoretical basis for these temperature-dependent frequency shifts is discussed below.

The next two figures show pertinent line-width data. Figure 19 gives the line width vs. the square of the exciton concentration. It may be noted that curve (a), for the pure sample, is quite linear, whereas curve (b), for the dirty sample, is not. Figure 20 is a plot of the difference in the line widths of the two samples vs. the exciton concentration. Figure 20 thus represents the free radical contribution to the total width in the dirty sample.

The exciton concentration, $\underline{c}$, used in Figures 19 and 20 was calculated according to the relation:

$$c \sim 3 \exp(-J/kT),$$

where $\underline{J}$ is the "activation energy" for the singlet-triplet transition as reported by Chesnut and Phillips (15) : $J = 0.062$ e.v.

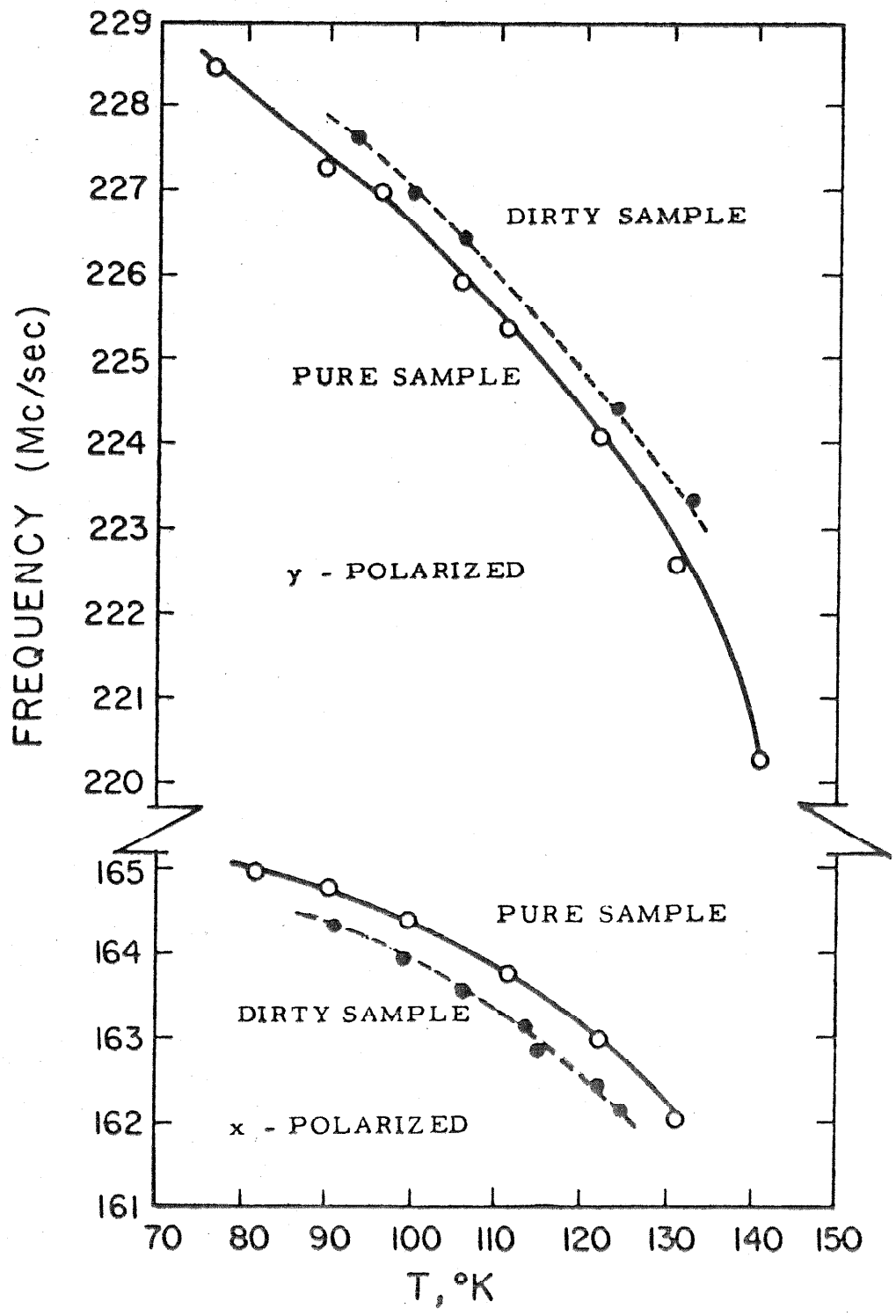

Figure 18. Temperature dependence of x and y transition frequencies in pure and "dirty" samples of $(\phi_3 As CH_3)^+(TCNQ)_2^-$ in zero field.

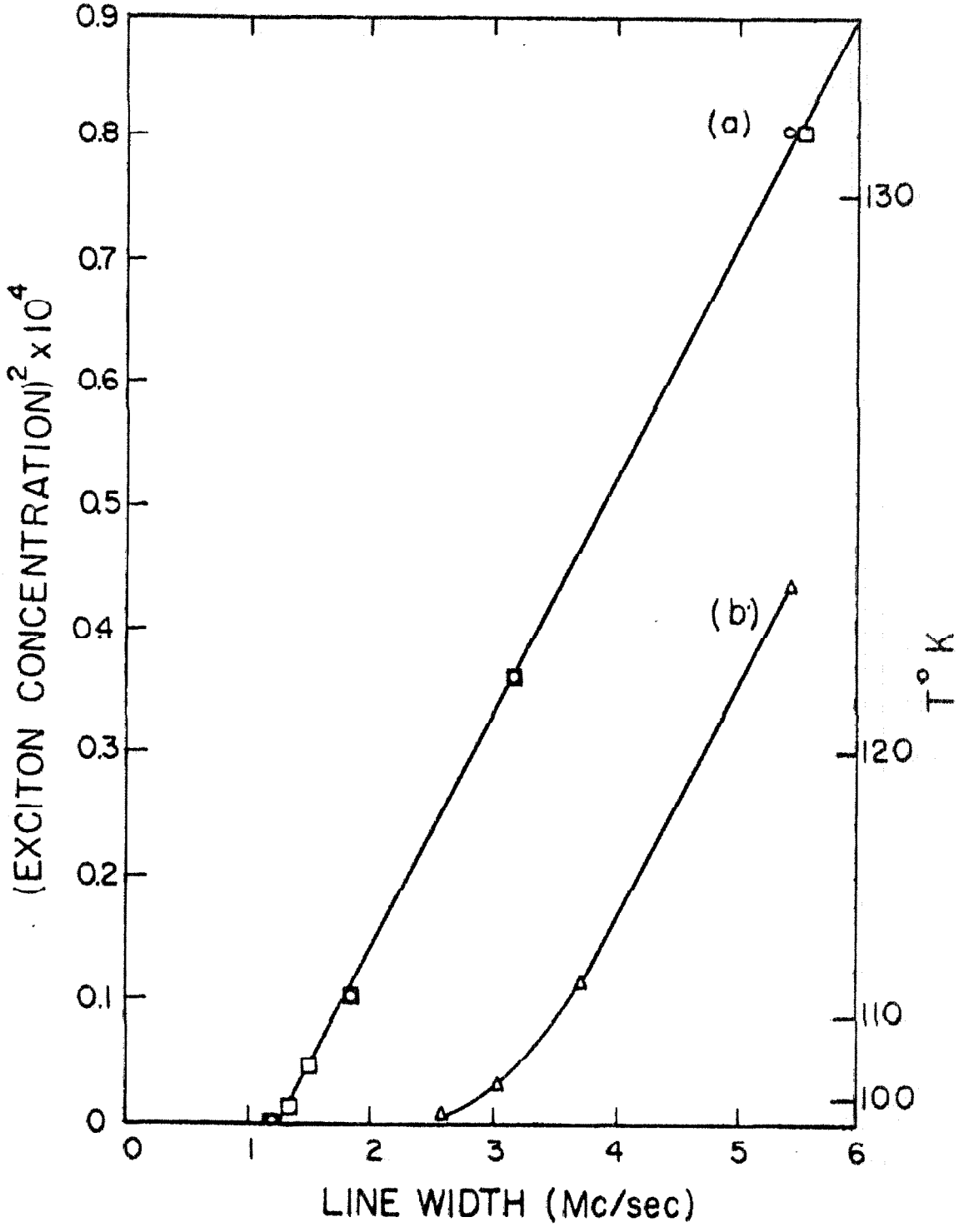

Figure 19. Relation between zero-field line widths in $(\phi_3 As CH_3)^+(TCNQ)_2^-$ and exciton concentration. Curve (a) gives line widths for the y-polarized transition (squares, □) and x-polarized transitions (circles, ○) in pure Sample I (see text), and curve (b) gives line widths for the y-polarized transition in dirty Sample II (see text).

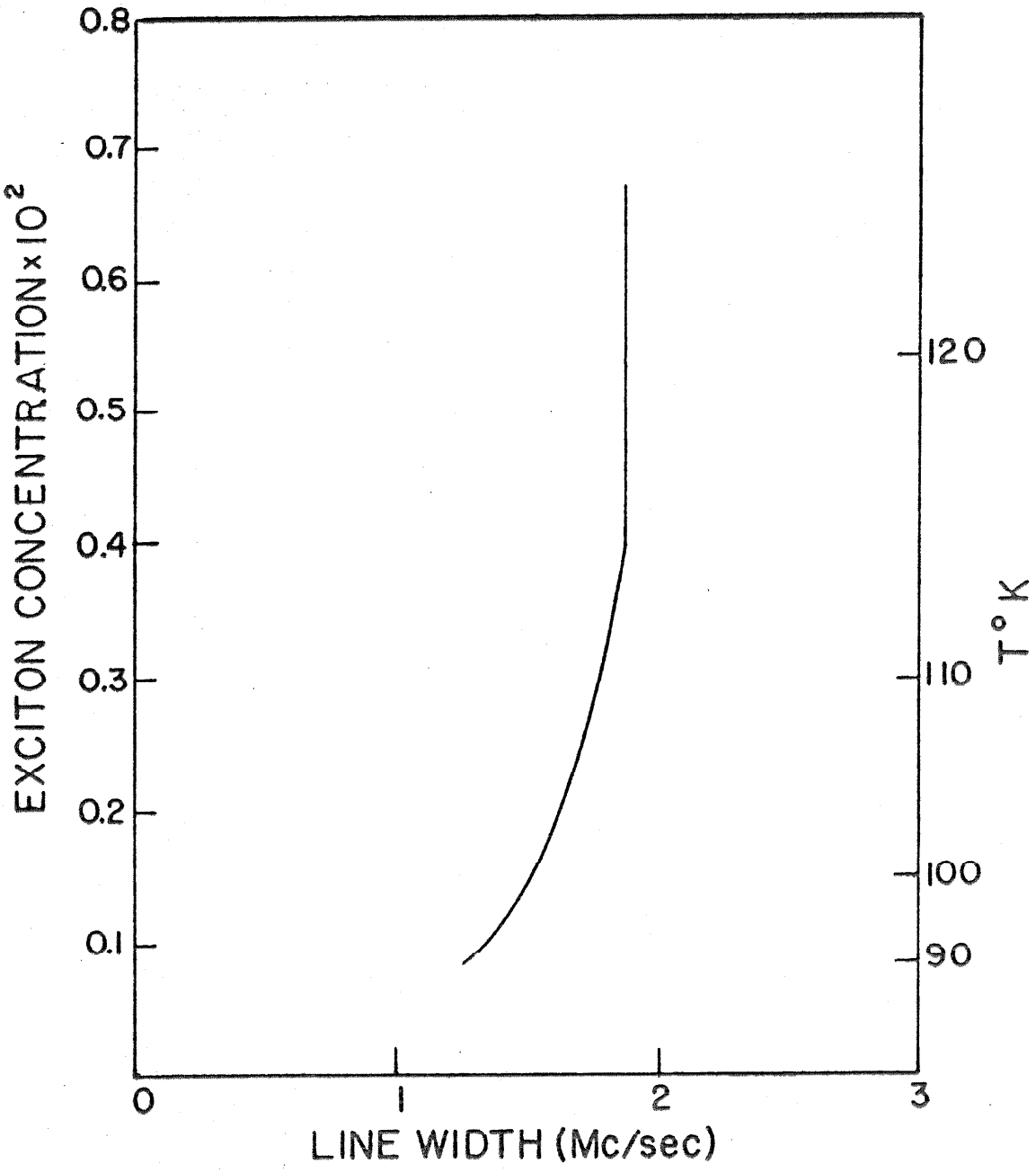

Figure 20. Calculated free radical contribution to the exciton line width in the "dirty" sample containing ca. 1% free-radical spin 1/2 impurities. The broadening is attributed to exchange interaction between excitons and the spin 1/2 free-radical impurities.

D. THEORETICAL DISCUSSION

The following section, in large part the work of Professor McConnell, has been taken verbatim from a paper which is being submitted for publication (21). Figure numbering and some notational changes have been made.

D - 1. FREQUENCY SHIFTS -- In this section we discuss the origin of the temperature dependence of the zero-field transition frequencies shown in Figure 18. First consider exchange contributions to the zero-field transition frequencies.

EXCHANGE INTERACTIONS -- Exchange interactions between excitons can give rise to shifts of the zero-field transition frequencies with increasing exciton concentration (i.e., increasing temperature). To understand this "exchange shift" let us consider two excitons of spin $S = 1$ that are coupled by an average "effective" exchange interaction J_{eff} that is small compared to the transition frequencies of the non-interacting excitons, ν_x, ν_y, ν_z. In zero field the spin Hamiltonian for the problem is

$$\sum_{i=1}^{2} X S_{ix}^2 + Y S_{iy}^2 + Z S_{iz}^2 + J_{eff} S_1 \cdot S_2 \quad . \tag{7}$$

Here $\nu_x = Y - Z$, $\nu_y = X - Z$, $\nu_z = X - Y$.

The first order effect of the exchange coupling of the excitons is to split each zero-field resonance into a triplet of equally spaced lines as illustrated in Figure 21 for the highest frequency transition ν_y.

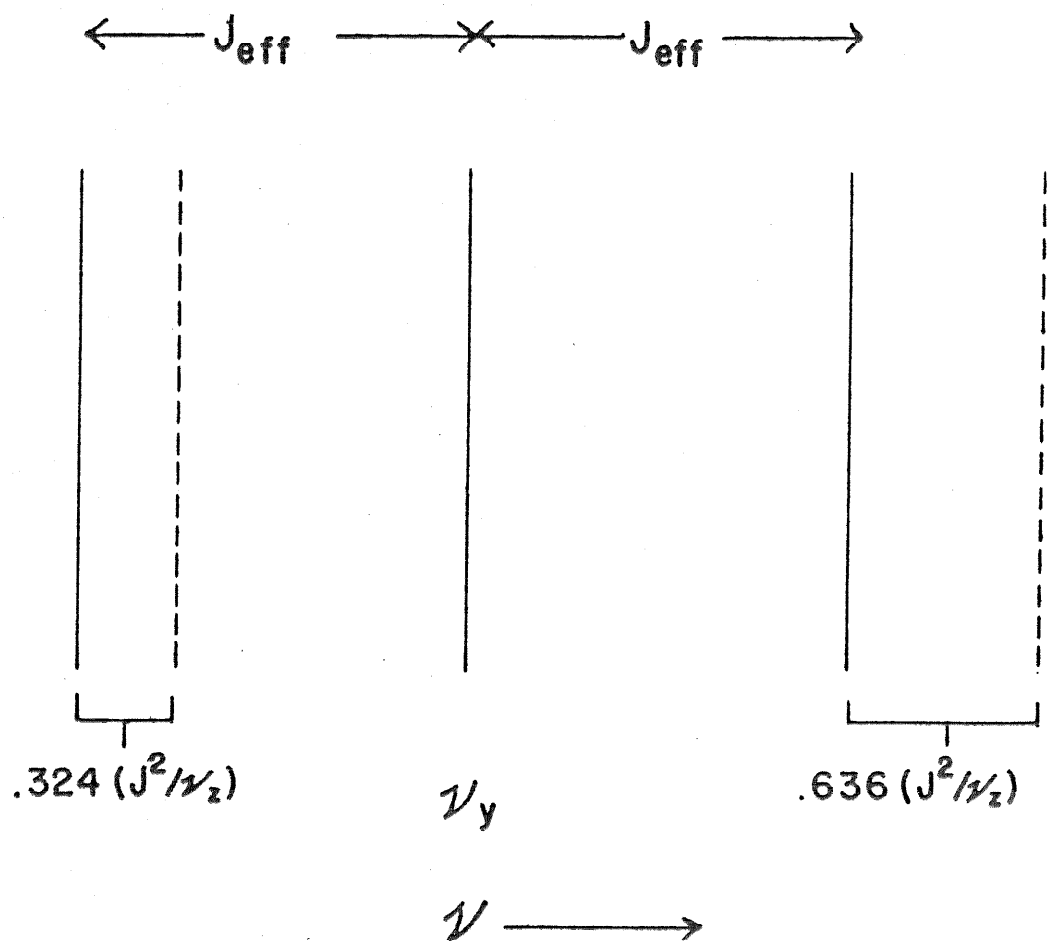

Figure 21. Exciton dimer spectrum. When two excitons are coupled by a weak exchange interaction, J_{eff}, the zero-field spectrum is split. The absorption at ν_y is split by first-order exchange interaction into three equally strong lines at $(\nu_y - J_{eff})$, ν_y, and $(\nu_y + J_{eff})$. The shift of the outer lines to higher frequencies by second-order exchange is shown by the dotted lines.

(This "exchange broadening" is discussed in more detail in the next section.) The second-order effects (as seen in Figure 21) produce a shift to higher frequencies. The average frequency for each of the transitions is readily found by second order perturbation theory:

$$\bar{\nu}_y = \nu_y + (2\nu_z/\nu_y + \nu_z/\nu_x + 1)\ J_{eff}^2/\ 6\nu_z$$

$$= \nu_y + 1.920\ (J_{eff}^2/6\nu_z)\ , \qquad (8a)$$

$$\bar{\nu}_x = \nu_x + (2\nu_z/\nu_x + \nu_z/\nu_y + 1)\ J_{eff}^2/\ 6\nu_z$$

$$= \nu_x + 0.024\ (J_{eff}^2/6\nu_z)\ , \qquad (8b)$$

$$\bar{\nu}_z = \nu_z + (\nu_z/\nu_y - \nu_z/\nu_x + 2)\ J_{eff}^2/6\nu_z$$

$$= \nu_z + 1.896\ (J_{eff}^2/6\nu_z)\ . \qquad (8c)$$

The numerical results above are based on the ratios $(\nu_z/\nu_y) \sim 60/220$ and $(\nu_z/\nu_x) \sim 60/160$.

Since increasing temperature corresponds to increasing exciton concentration and increasing the effective exchange interaction, J_{eff}, between the excitons, the observed decrease of, for example, ν_y with increasing temperature cannot be accounted for by the exchange effect since this effect produces a shift to higher frequencies. Moreover, the order of magnitude of the calculated exchange shift is too small. For example, consider the y-polarized transition in pure Sample I in the lower temperature region (80 - 110 ^{o}K). The experimental value

for the temperature dependence of the transition frequency is

$$\left(\frac{1}{\nu}\frac{d\nu}{dT}\right)_{expt} \sim 3 \times 10^{-4} \quad (^{o}K)^{-1} . \qquad (9)$$

The exchange contribution to $\frac{1}{\nu}\frac{d\nu}{dT}$ is of the order

$$\left(\frac{1}{\nu}\frac{d\nu}{dT}\right)_{exch} \sim 2 \quad \frac{J_{eff}}{\nu^2} \quad \frac{d\,J_{eff}}{dT} \qquad (10)$$

$$\sim 1.5 \times 10^{-6} \quad (^{o}K)^{-1}$$

in the temperature range 80 - 100 °K, where the observed line width is taken equal to J_{eff} ($\sim$1.5 Mc/sec) and (dJ_{eff}/dT) is estimated to be $\sim 2 \times 10^{-2}$ Mc/sec $(^{o}K)^{-1}$ from the temperature dependence of the line width. The exchange contribution to the shift must be even less than 1.5×10^{-6} $(^{o}K)^{-1}$ since the line width must have contributions other than first-order exchange (see below). Thus, in the 80 - 110 °K range, exchange interactions make no significant contribution to the observed temperature dependence of the transition frequencies. In the earlier high-field study of $(\phi_3 As CH_3)^+ (TCNQ)_2^-$ Jones and Chesnut (17) have also noted that the temperature dependence of the fine-structure splitting could not be accounted for in terms of exchange interaction between excitons.

Exchange interactions between spin 1/2 impurity free radicals and triplet excitons can also produce second-order exchange shifts. Exchange interactions between excitons and free-radical impurities

have been previously noted in high-field spectra (22). For example, if we consider a triplet exciton , exchange coupled with a free electron spin through a weak exchange interaction J_{eff} , then we may calculate the following average transition frequencies for the exciton-free electron spin complex in zero field:

$$\bar{\nu}_y = \nu_y + 1.920 \left(J_{eff}^2 / 4\nu_z \right) , \quad \text{(11a)}$$

$$\bar{\nu}_x = \nu_x + 0.024 \left(J_{eff}^2 / 4\nu_z \right) , \quad \text{(11b)}$$

$$\bar{\nu}_z = \nu_z + 1.896 \left(J_{eff}^2 / 4\nu_z \right) . \quad \text{(11c)}$$

The exchange shifts given in the above expressions are based on the frequency ratios: $(\nu_z / \nu_x) \sim 60/160$ and $(\nu_z / \nu_y) \sim 60/220$. We suggest that the frequency shifts of "dirty" sample II relative to "pure" sample I may be due to second-order exchange interaction between the exciton and the impurity free radicals. Unfortunately, this is not simply an exciton-spin 1/2 interaction problem, because for a realistic calculation one must consider the (very complicated) zero-field states of the free radical due to hyperfine interactions. Even the signs of the exchange shifts are difficult to predict when the frequency separations of the zero-field hyperfine states are comparable to those of the triplet exciton, which is very probably the case in the present problem. For zero-field hyperfine states that have separations less than exciton fine-structure states, one does not expect a second-order shift of the highest frequency exciton transition to still higher frequencies, as observed.

The data in Figure 20 suggest that the exchange broadening of the exciton resonance is roughly independent of temperature and exciton concentration. This indicates the absence of a large activation barrier to exciton-free radical exchange interaction. This point is discussed in more detail later.

EXCITON MOTION -- It is shown elsewhere (11) that the spin Hamiltonian, and hence the zero-field transition frequencies, of a triplet exciton depend on the wave vector $\vec{k}$. When exciton bands are narrow compared to thermal energies all k-states are populated with nearly equal probability, and the temperature dependence of the transition frequencies due to this effect can be neglected. We shall assume that the exciton band in $(\phi_3 As CH_3)^+(TCNQ)_2^-$ is indeed this narrow.

TORSIONAL MOLECULAR OSCILLATIONS -- The temperature dependence of nuclear quadrupole frequencies in crystals of chlorinated aromatic molecules is qualitatively similar to the temperature dependence of the zero-field transition frequencies of $(\phi_3 As CH_3)^+(TCNQ)_2^-$ shown in Figure 18. For example, in the temperature region 170 - 270 ^oK the chlorine quadrupole resonance frequency in chlorobenzene at 34 - 34.5 Mc/sec decreases at a rate of the order of $\frac{1}{\nu}\frac{d\nu}{dT} \sim -10^{-4}(^oK)^{-1}$. It is well known that this temperature dependence of the quadrupole frequency in aromatic crystals is due largely to torsional molecular motion (23), and it is exceedingly likely that this motion is also responsible for most of the temperature dependence of

the zero-field transition frequencies seen in Figure 18 in the 80 - 110 °K region. Since the theory of the effect of torsional motion on nuclear quadrupole frequencies can be carried over to the exciton problem with almost trivial modifications, we shall not present a detailed discussion except to point out that a realistic order-of-magnitude calculation can be made.

For simplicity consider two coaxial benzene negative ions on top of one another, as sketched in Figure 22, with uniform spin densities of $\rho_i = 1/6$ on each carbon atom. The spin Hamiltonian for this symmetry is of the form DS_z^2, where D is given by the following formula (19) which only includes contributions from nearest neighbor intermolecular carbon-carbon pairs:

$$D = 3/4\ g^2\beta^2 \sum \rho_i^2 (1 - 3\cos^2 \Theta_i) R_i^{-3} . \quad (12)$$

Here Θ_i is the angle between the instantaneous nearest neighbor intermolecular carbon-carbon vector $\vec{R}_i$ and the axis of the two rings. Again for simplicity of calculation we take as equilibrium configuration one in which the carbon atoms are directly above one another. Then for small oscillations of the rings about this common axis (Θ small) one obtains the following expression,

$$\frac{1}{D}\frac{dD}{dT} = -3\ \frac{d\langle\Theta^2\rangle}{dT} , \quad (13)$$

where $\langle\Theta^2\rangle$ denotes the thermal average of Θ^2. In the classical limit,

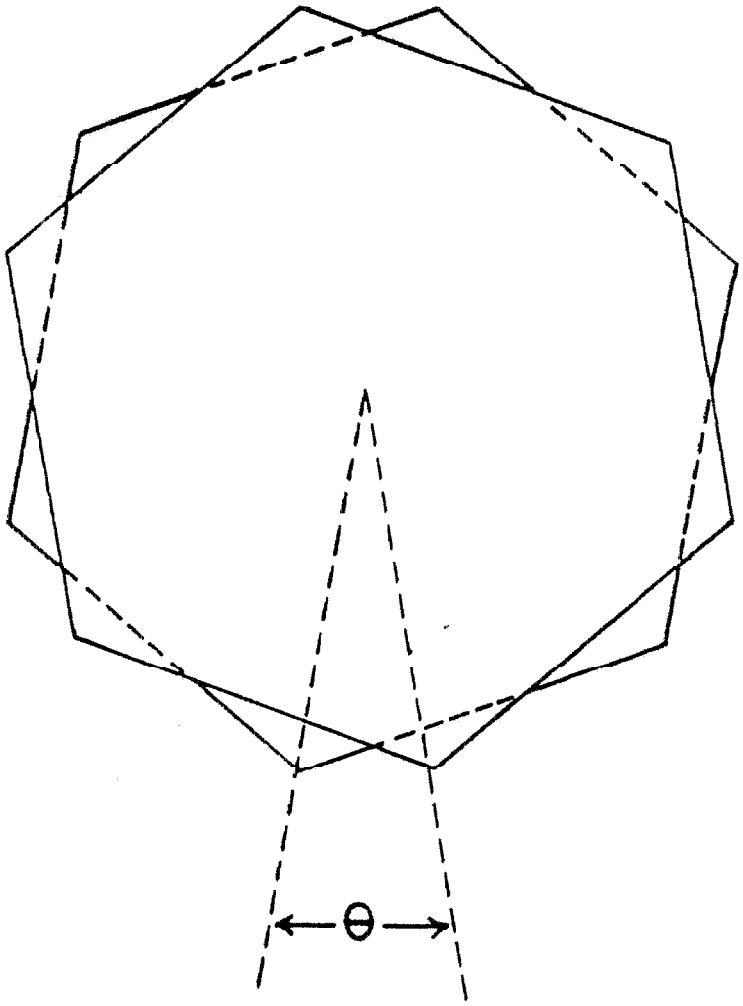

Figure 22. Model used for the calculation of the temperature dependence of the zero-field transition frequencies due to molecular torsional motion. Two coaxial benzene negative tions with uniform spin density oscillate through an angle θ relative to each other.

$kT \gg \hbar\omega$, where ω is the torsional oscillation frequency, $\langle\theta^2\rangle$ is proportional to the absolute temperature(23), $\langle\theta^2\rangle = \lambda T$. The order of magnitude of $\langle\theta^2\rangle$ can be inferred from r.m.s. thermal parameters observed in X-ray diffraction spectra. Although these data are not available for $(\phi_3 As CH_3)^+ (TCNQ)_2^-$, experimental studies on other charge-transfer type crystalline complexes (24) show the mean square deviation of peripheral atoms to be as high as 0.08 $A^{o\,2}$ at room temperature. This deviation corresponds to a λ of the order of 0.08/300 or 2.7×10^{-4}. Thus, we obtain the estimate

$$\frac{1}{D}\frac{dD}{dT} \sim -8 \times 10^{-4} \ (^oK)^{-1} , \qquad (14)$$

which is in satisfactory order-of-magnitude agreement with the experimental temperature dependence of the zero-field transition frequencies.

D - 2. RESONANCE LINE WIDTHS

The temperature dependence of the high-field exciton magnetic resonance line width in $(\phi_3 As CH_3)^+ (TCNQ)_2^-$ has been previously studied by Chesnut and Phillips (15), and Jones and Chesnut (17). In the present section we compare the high-field and zero-field line widths and consider briefly the origin of these widths in terms of exciton structure and motion.

At low temperatures ($\sim 77^oK$) the high-field exciton resonance lines are Lorentzian, with line widths in the range 1.1 $\rightarrow$ 3.3 Mc/sec (25) depending upon the crystal orientation relative to the applied field

direction. This anisotropy may be due to exciton-nuclear hyperfine interactions that are not completely averaged out by exciton motion. This hyperfine interaction should not contribute to the zero-field line widths, since in zero field the hyperfine interaction is second-order, whereas it is first order in high fields. The zero-field width of about 1.25 Mc/sec at $\sim 77^{\circ}K$ is thus consistent with the narrowest high field width, 1.1 Mc/sec (25) obtained at this temperature, provided that the first-order high-field interaction can be neglected at this orientation.

To understand the possible significance of these results, let us tentatively assume a diffusional model in which a localized exciton hops from site to site on the linear free-radical chain with jumping probability τ^{-1}. In a time t the exciton makes t/τ jumps, and moves over a number of distinct sites n, where $n \sim (t/\tau)^{1/2}$. The high-field hyperfine line width W_{hf} of an exciton distributed over n sites is of order $A/n^{1/2}$ where A is the hyperfine line width of an exciton localized on a single site. Thus,

$$W_{hf} \sim A\,(\tau/t)^{1/4}. \tag{15}$$

We set $t = W_{hf}^{-1}$ since this is essentially the life time of the magnetic state giving the observed resonance. This leads to the result

$$\tau^{-1} \sim A^4/W_{hf}^{3}. \tag{16}$$

Since A is estimated (11) to be of the order of 30/Mc/sec and W_{hf} above is estimated to be of the order of 1 Mc/sec, we obtain $\tau^{-1} \sim 10^{11}$-10^{12}.

Within a time of order $(1\ \text{Mc/sec})^{-1}$, the jumping exciton covers a distance of order 10^{13} sites. This indicates that at an exciton concentration of the order of 10^{-3} one may see a line broadening process of the order of 1 Mc/sec due to exchange collisions between the excitons, if every collision is effective for line broadening (no barrier). The increase in line width by 1 Mc/sec (above the low temperature limiting line width) with increasing temperature does set in at an exciton concentration of about 3×10^{-3} in the zero-field data given for the pure sample in Figure 19, and also occurs at the same place in high-field resonance data.

There is an important difficulty with the simple discussion given above. The exciton line width is not simply proportional to the exciton concentration, as seen from Figure 19. In Figure 19 the zero-field line width has been plotted against the square of the exciton concentration for convenience in extrapolating to zero exciton concentration; the nearly quadratic relationship of this type is not general for other exciton containing solids (17, 19). In previous work (18) it has been suggested that the exciton line width may increase more rapidly than the exciton concentration itself due to a phonon-coupled repulsion between excitons that leads to an activation barrier for exciton-exciton exchange interaction. (For $[\phi_3 As CH_3]^+[TCNQ]_2^-$ this barrier must then be accidentally equal to the exciton excitation energy itself.) Thus, at an exciton concentration of the order of 10^{-3}, only a fraction of the order of 10^{-3} of all collisions are then effective in producing broadening.

This mechanism would then seem to be inadequate to account for the exchange broadening in Figure 19, especially at low exciton concentrations (26).

Collisions between two diffusing excitons are not the only mechanism for exciton-exciton exchange broadening, however. It is quite reasonable to imagine that the following process of exciton creation and annihilation is quite rapid, since spin is conserved.

$$\text{exciton} + \text{exciton} \rightleftharpoons \text{exciton} + \text{phonons} .$$

In this process excitons are created and annihilated adjacent to already existing excitons. The rate of exciton diffusion is thus not directly connected to the rate of this exchange broadening process. This creation interaction can be expected to proceed at a rate W_c of the order

$$W_c \sim \Gamma \exp(-\beta J) \cdot \exp(-\beta V_2)$$

where V_2 is the phonon-coupled repulsion (18) between two adjacent localized excitons. Here Γ is a rate constant for the interconversion of exchange and lattice energy, which might be as large as 10^{12}/sec since the energy transformed between the exchange and lattice system is rather small ($J \sim 500\ cm^{-1}$), and the energy transfer does not require a change of spin multiplicity. For this Γ the creation interaction leads to a line width of the order of 1 Mc/sec when the exciton concentration is of the order of 10^{-3} and the barrier V_2 is approximately equal to J. If this mechanism for line broadening were correct,

it would account for the observed dependence of line width on temperature.

The apparent constancy of the contribution of exciton-free radical exchange interaction to exciton line broadening seen in Figure 20 for exciton concentrations above ca. 3×10^{-3} is precisely what is expected when there is no significant activation barrier to exciton interaction with the free radical impurity. This result is consistent with the approximate constancy of the second-order exchange shift due to exciton-free radical interactions seen in Figure 19. The decrease of this line width at the lower concentrations is not expected or understood. It might arise from a small barrier to exciton-free radical interaction.

The foregoing discussion of line widths is obviously crude, incomplete, and tentative. On the other hand, exciton line widths probably will provide the best key to an understanding of exciton structure and motion in solid free radicals, and the foregoing estimates are certainly better than none at all in the absence of a comprehensive theoretical treatment.

REFERENCES

1. Terman, Electronic and Radio Engineering, McGraw-Hill Book Company, New York (1955).
   Seely, Electron-tube Circuits, McGraw-Hill Book Company, New York (1953).
   Langford-Smith, Radiotron Designer's Handbook, Radio Corporation of America, Harrison, N. J., (1953).

2. Cole, Kushida, and Heller, J. Chem. Phys., 38, 3915 (1963).

3. Kojima, Shimauchi, Hagiwara, and Abe, J. Phys. Soc. Japan, 10, 930 (1955).

4. Massachusetts Institute of Technology, Radiation Laboratory Series, Mc-Graw-Hill Book Company, New York (1948).

5. Complete technical information may be obtained from General Electric, manufacturer of the Nuvistor tubes.

6. General Electric, Tunnel Diode Manual, G. E., Liverpool, N. Y. (1961).

7. D. B. Chesnut and W. D. Phillips, J. Chem. Phys., 35, 1002, (1961).

8. R. C. LaForce, Rev. Sci. Instr., 32, 1387 (1961).

9. Wheatley, Griffing, and Estle, Rev. Sci. Instr., 27, 1070 (1956).

10. Verdieck and Cornwell, Rev. Sci. Instr., 32, 1383 (1961).

11. H. M. McConnell and R. Lynden-Bell, J. Chem. Phys., 36, 2393 (1962).

12. R. Lynden-Bell and H. M. McConnell, J. Chem. Phys., 37, 794 (1962).

13. Frenkel, Phys. Rev., 37, 17(1931).

14. Davydov, Theory of Molecular Excitons, McGraw-Hill Book Company, New York (1962).

15. Chesnut and Phillips, J. Chem. Phys., 35, 1002 (1961).

16. Chesnut and Arthur, J. Chem. Phys., 36, 2969 (1962).

17. Jones and Chesnut, J. Chem. Phys., 38, 1311 (1963).

18. H. M. McConnell and Z. Soos, J. Chem. Phys., in press.

19. Thomas, Keller, and McConnell, J. Chem. Phys., 39 2321 (1963).

20. Stevens, Proc. Royal Soc. (London), A 214, 237 (1952).

21. Thomas, Merkl, Hildebrandt, and McConnell, being prepared for publication.

22. McConnell, Griffith, and Pooley, J. Chem. Phys., 36, 2518 (1962).

23. See, for example, H. Bayer, Z. Physik,131, 227 (1951), and Kushida, Benedek, and Bloembergen, Phys. Rev., 104, 1364 (1956) and further references contained therein.

24. See, for example, Harding and Wallwork, Acta Cryst. 8, 787, (1955) and Jones and Marsh, Acta Cryst. 15, 809 (1962).

25. The existence of this anisotropy was originally noted by D. Chesnut (private communication). The numerical values quoted here are from unpublished measurements of Griffith, Keller, and McConnell.

26. A detailed theory of resonance line broadening due to exchange collisions between diffusing excitons (spin = 1) has been developed by R. Lynden-Bell, Mol. Phys., in press.

PROPOSITION I

Various studies (1, 2, 3) have been made of the dependence of the electric quadrupole resonance frequency on pressure and temperature. In particular, the work of Kushida, Benedek, and Bloembergen (3) was performed in temperature ranges from $\sim -77^{\circ}C$ to $\sim +80^{\circ}C$, at pressures of one to ten thousand atmospheres. Their spectrometer was of the familiar Pound-Watkins type (4). The use of a high-pressure bomb necessitates the use of long electrical leads for bringing the radio-frequency power to the coil, which is enclosed in the bomb. At lower frequencies (probably less than ca. 40 Mc/sec) the additional capacitance and inductance of the leads, although by no means negligible, is small enough to allow a tuning range of several megacycles. Since $1/\nu \ (\partial\nu/\partial P)_T \sim 6 \times 10^{-8}$ for the compounds observed, a tuning range of only a few tenths of a megacycle is adequate for pressure experiments run at pressures up to 10 kilobars.

Recently some work of unknown extent has been started with spectrometers working at higher frequencies (5). In this work, the radio frequency line which goes through the wall of the pressure bomb is part of a matched transmission line. A transmission line, however, is matched exactly at one frequency, and is only approximately matched for nearby frequencies. The possible tuning range in this set up is undoubtedly quite small.

In view of the above considerations it was decided to investigate the possibility of designing an oscillator with a wide tuning range that could be used to study the pressure effects up to pressures of the order of 10 kilobars. It was decided to use the pressure bomb itself as part of the spectrometer system.

The design shown in Figure P-1-1, P-1-2, and P-1-3 show the essential elements of such a spectrometer. The proposed frequency range to be covered is 125-400 Mc/sec. It is expected that the whole range can be scanned with a maximum of two adjustments of the plate line, the change in the plate line in no way affecting the sample-containing pressure bomb. A plate line that will work with the spectrometer is shown in Figure 2 of this thesis. The top plug is the standard Bridgman plug (6). The conical electrical feed-through has recently been described (7).

In addition to the pressure and temperature dependence of the quadrupole frequencies, it will be worthwhile to study effects of high pressure on the spin resonance of triplet exciton systems. D and E (See Part II of thesis) are very sensitive functions of the intermolecular forces and, therefore, distances. Large effects in the resonance frequencies will surely be obtained(Kushida and Cole have mentioned that organic crystals, which they have subjected to these large hydrostatic pressures, were reduced in size by 30%!)

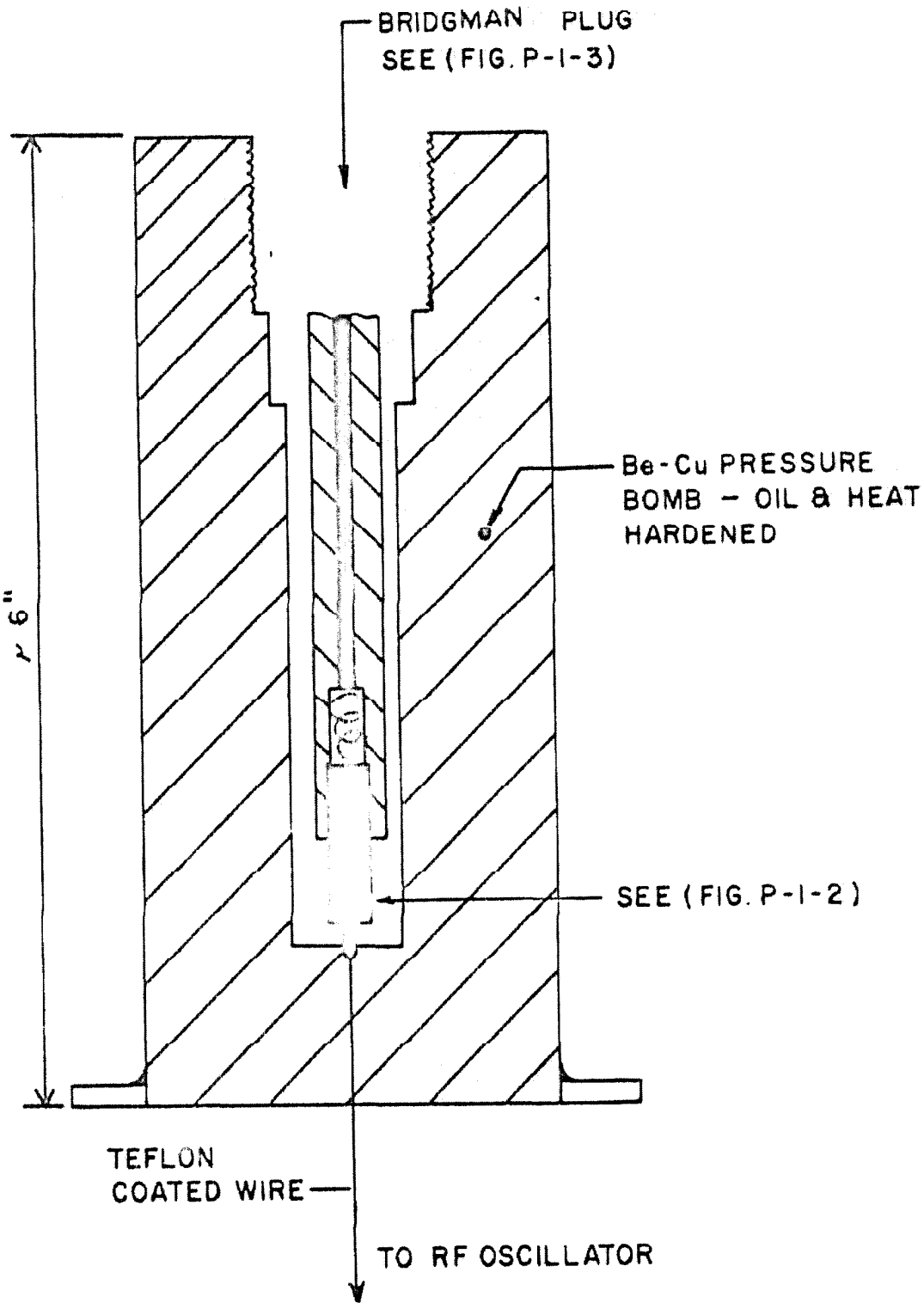

Figure P-1-1. Coaxial-line Pressure Bomb.

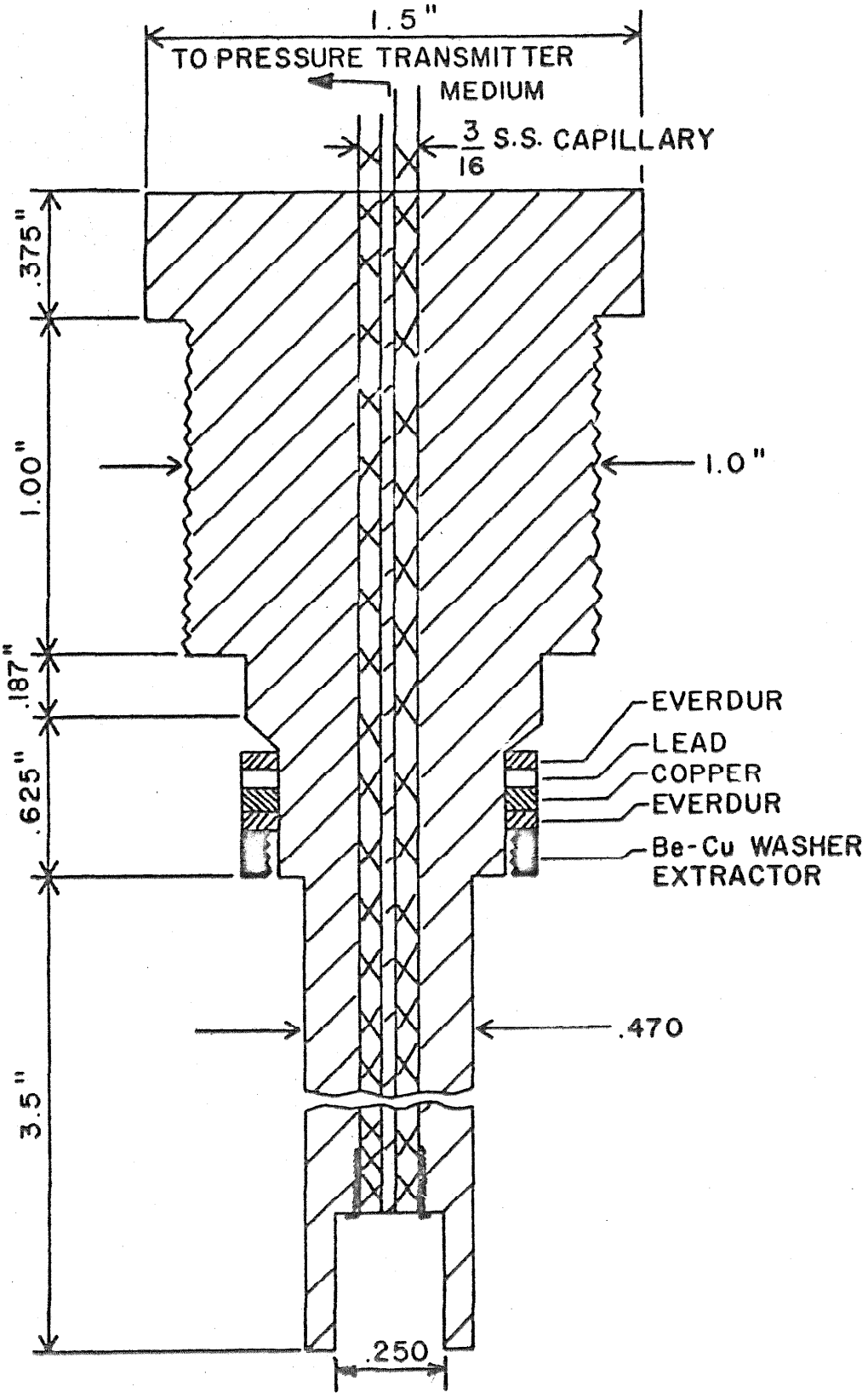

Figure P-1-2. Bridgman plug - center coax line.

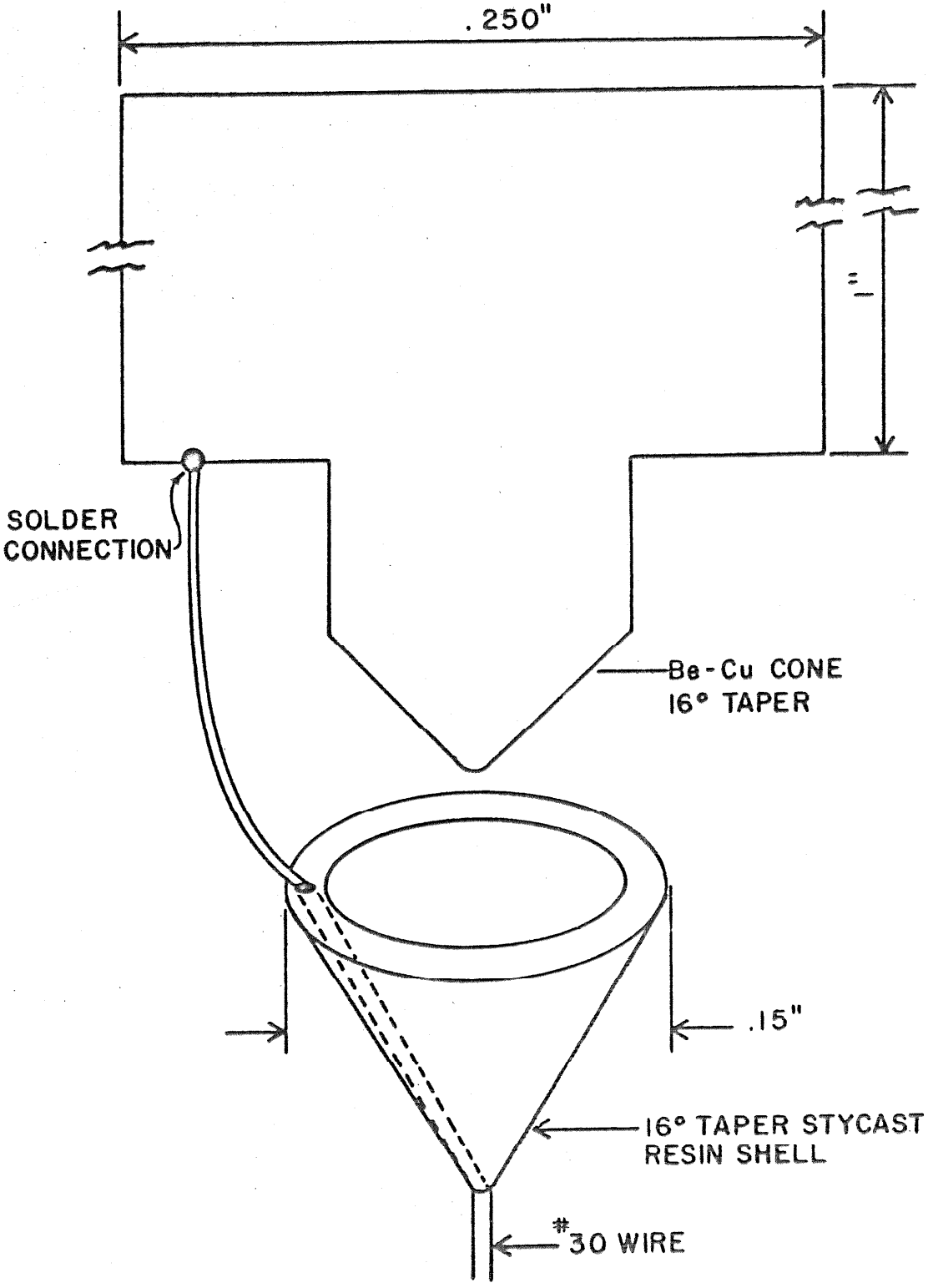

Figure P-1 3. Conical seal - electrical feed-through.

PROPOSITION II

Hutchison and Mangum (8) observed the paramagnetic resonance absorption of phosphorescent naphthalene in solid solutions of durene. They reported that all their experiments gave results explicable by the spin Hamiltonian

$$\mathcal{H} = g\beta \mathbf{H}\mathbf{S} + D S_z^2 + E (S_x^2 - S_y^2),$$

where $S = 1$, $g = 2.0133$; $D/hc = -0.1003$, and $E/hc = 0.0140$ cm^{-1}.

McConnell suggested that a study of the possible microwave modulation of phosphorescence (MMOP) be made. A few preliminary experiments during this past year endeavored to observe the changes in intensity and/or polarization of the phosphorescence of naphthalene in durene during the process of paramagnetic resonance. No results were obtained; the experiments were all performed in high fields.

In the absence of large magnetic fields, the Zeeman term of the above Hamiltonian disappears, and we are left with the familiar D and E Hamiltonian. Direct absorption of microwave power by triplets in naphthalene in durene will occur at the frequencies, (D+E), (D-E), and 2E. The first two transitions are centered at $\sim$3000 Mc/sec.

The radio-frequency power source (9) illustrated in Figure P-2-1 is suggested for the MMOP experiment. The experimental arrangement proposed is the following. The central section of the microwave

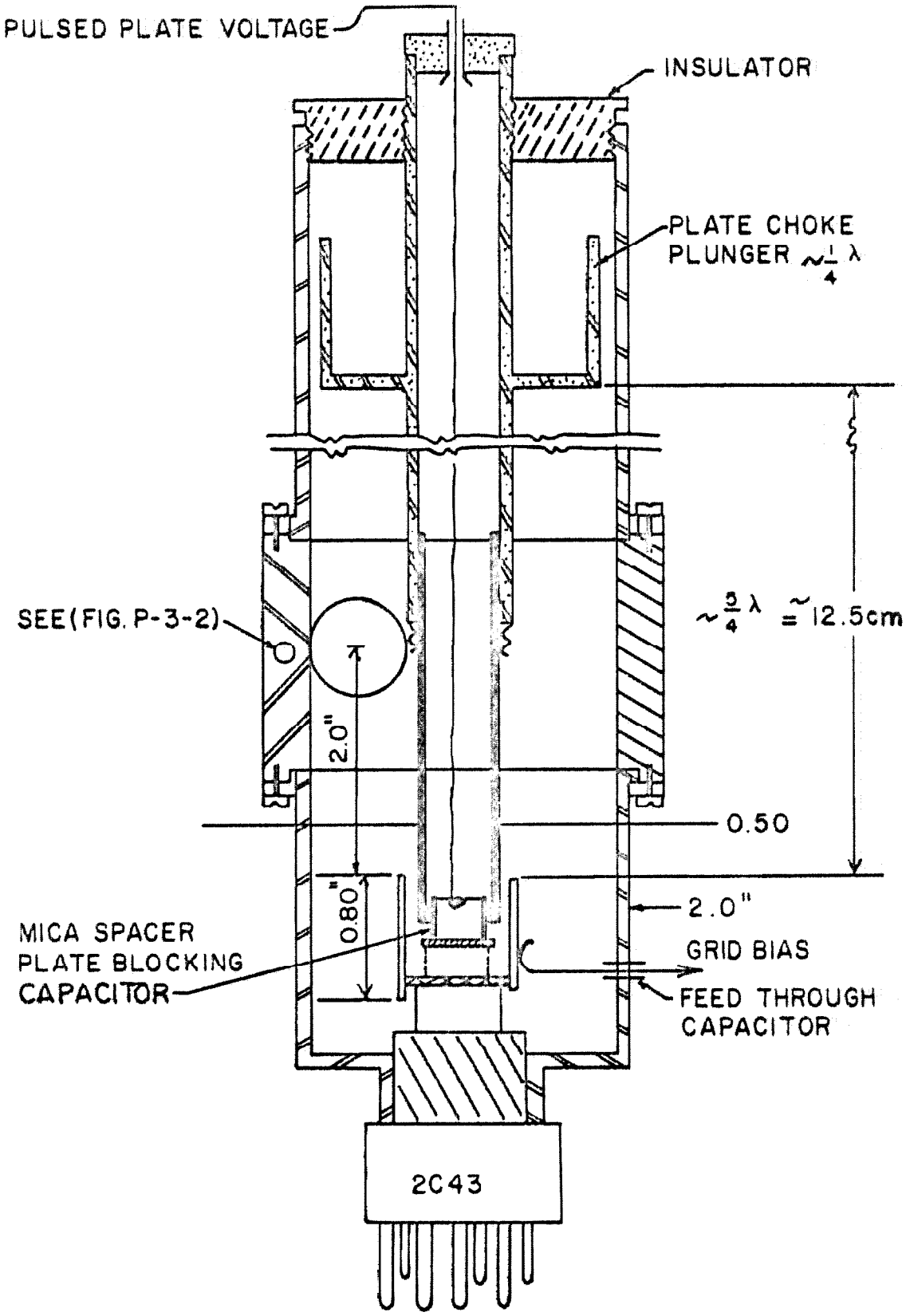

P-2-1. Microwave generator for modulation of phosphorescence.

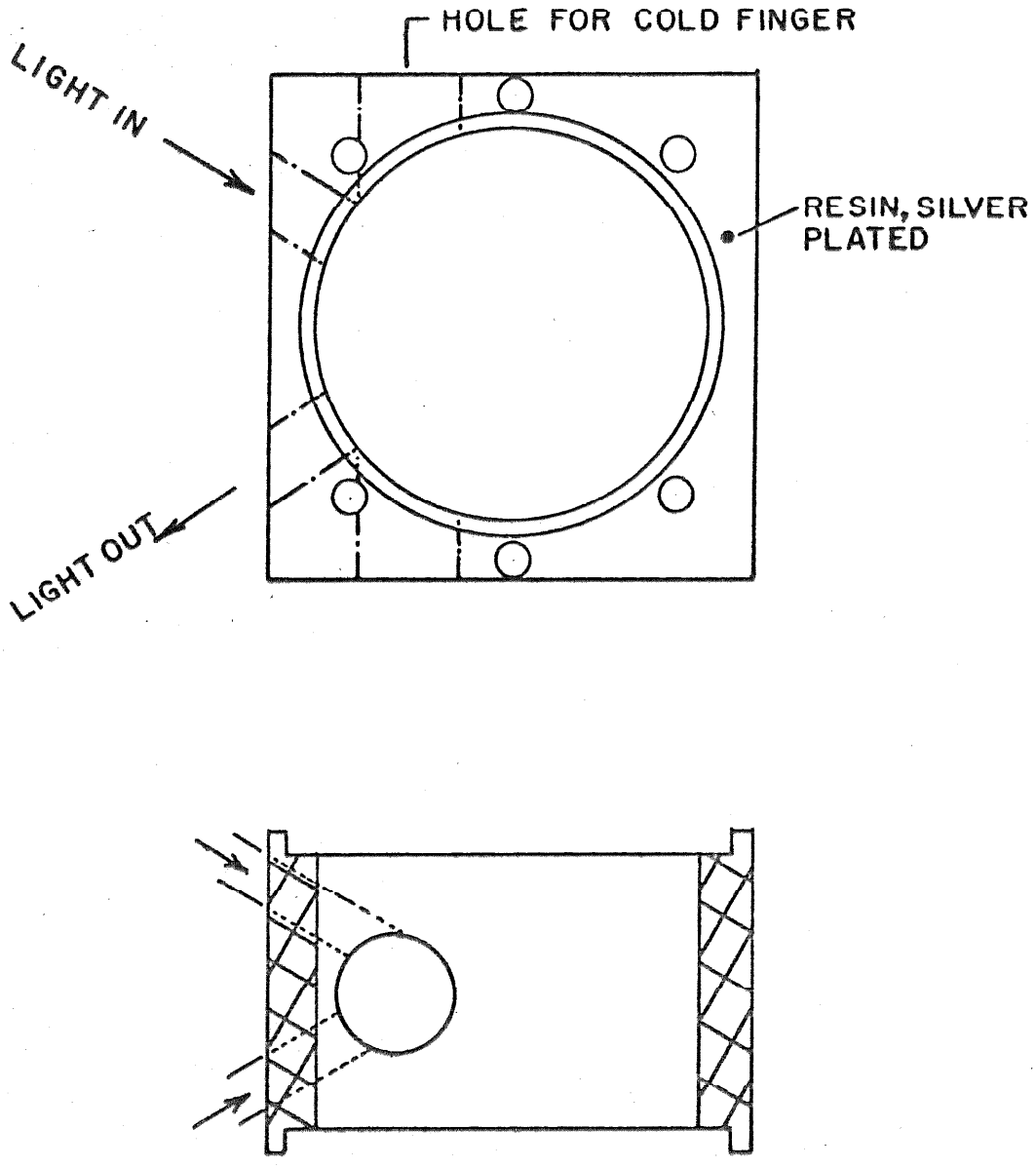

Figure P-2-2. Center section of outer coaxial line.

generator (see Figure P-2-2) has three holes in it. The sample-containing cold finger is put into the hole designated in Figure P-2-2, which corresponds to a point of maximum magnetic field ($\lambda/2$). The other holes allow irradiation and observation of the sample. Because the effect will be modulated at an A.C. rate (see below), it should be possible to detect small changes in intensity and/or polarization.

The following comparative listing of experimental conditions shows possible advantages of the proposed system:

a) The microwave source shown in Figure P-2-1 is easily pulsed, with peak powers of the order of 100 watts; the power available in the present spectrometer system is limited to ca. 100 milliwatts. For initial experiments along this line, the large power levels should be a distinct advantage.

b) Since the proposed system is pulsed, the phosphorescent spectrum will be modulated at the pulse frequency; to obtain modulation with the currently available Varian system, it is necessary to use magnetic field modulation. Large modulation fields are not readily attainable, and there are many pick-up problems associated with them (e.g., the photomultiplier tube).

c) Since the proposed system is to be run in zero field, the problems caused by the anisotropy of the magnetic splittings are eliminated.

PROPOSITION III

The resonance frequencies and the line widths of triplet excitons are very sensitive functions of temperature (10). In addition, the paramagnetic — diamagnetic transition temperature of solid-free radical systems is variable. Hence the need for a system which will operate over a wide temperature range.

Figure P-3 is a cross sectional view of a proposed design for a dewar-coaxial line cavity. The design is flexible, and by varying relative line dimensions, it should be applicable for use over a wide frequency range.

Any size flanges may be fixed to the top end, facilitating connection to existing Helium dewars. The bottom plate (epoxy sheet, in Figure P-3) may be made of any insulator strong enough to withhold the pressure differential. The radio frequency connection is made through this insulator to the center coaxial line, which also serves as the cold finger (metal). The indium seal at the top end of the cold finger provides both the vacuum seal for Helium as well as a current path to the stainless steel (or Be-Cu) shield which also serves as the return conductor. The sample region is defined by the inner cold finger and the indicated glass wall. The spring in the center line provides for mechanical rigidity needed to eliminate noisy, intermittent electrical contact, as well as the necessary compensation for the different

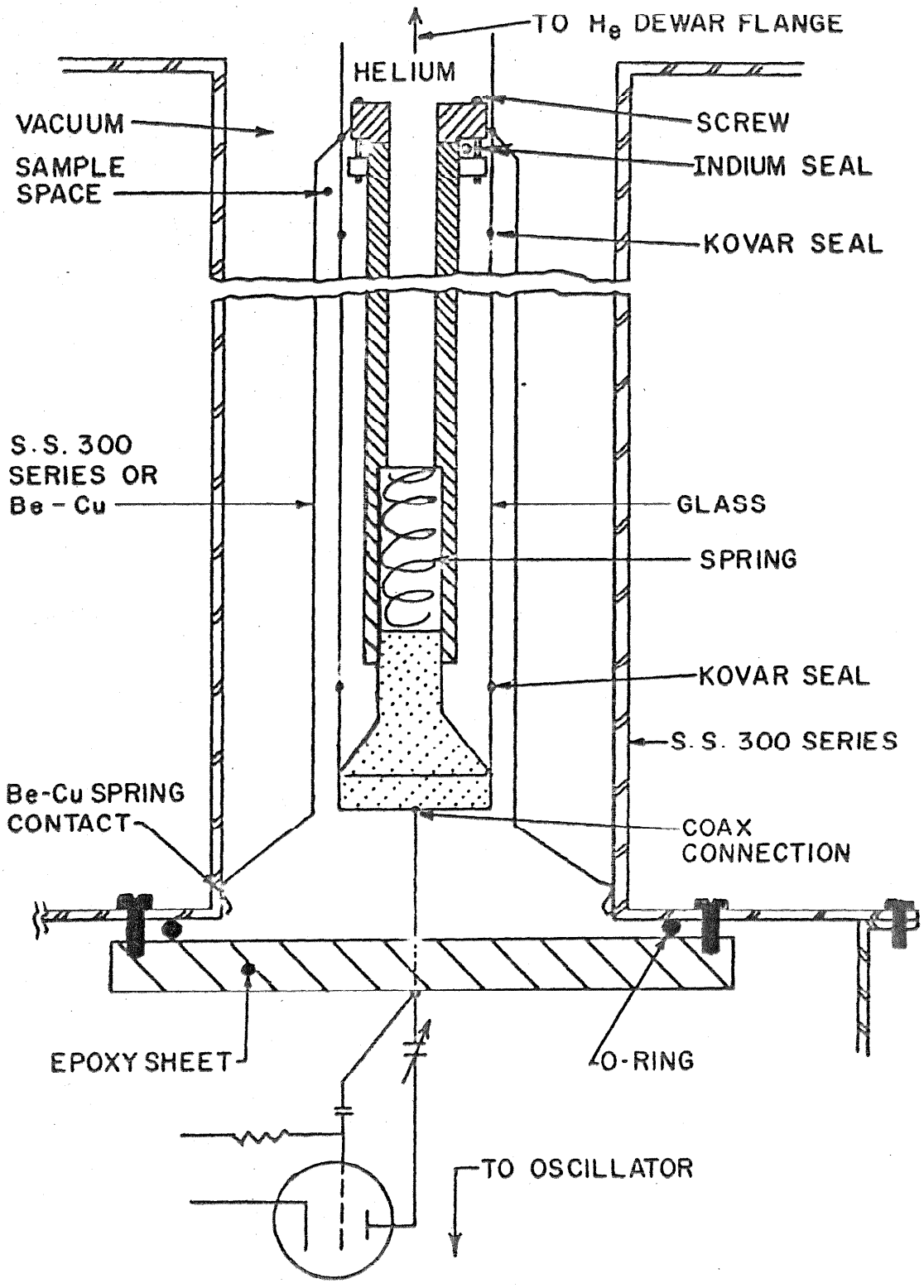

Figure P-3 Coaxial cavity attachment for low temperature work.

expansion coefficients of the metal center line and the glass wall.

Helium Losses: The feed-through wire attached to the bottom of the cold finger can be of quite small diameter and heat losses will be insignificant. The stainless or Be-Cu shield (return path for radio frequency current) makes contact with the helium cold finger (on top) and the room temperature outter wall (on the bottom). Below $50^{o}K$ an additional heat shield, one made of quartz maintained at approximately $77^{o}K$ may be placed between the outer wall and the stainless line. Heat losses due to electrical heating are small (if all electrical energy were dissipated in this line, the loss would be approximately 1/10 liter per hour of liquid helium).

PROPOSITION IV

Frequency-modulated spectrometers have found fairly wide use in nuclear electric quadrupole resonance work. Typical quadrupole resonances are of the order of kilocycles wide, and there is no great problem in modulating through the whole line width with one sweep.

Electron resonance lines, nuclear magnetic resonance lines in ferromagnets, as well as the resonances observed in triplet exciton systems, however, are generally of the order of several megacycles wide (11).

A widely accepted method of frequency modulation involves the use of varicaps (a diode, whose capacitance is a function of the bias voltage). These circuit elements may be schematically replaced by a series resistor and capacitor, the internal resistance of the diode being approximately independent of the capacity. A change in diode bias causes an obvious variation in the capacitance/resistance ratio of the diode. This causes a change in the Q of the resonant circuit, irrespective of the frequency dependence of the reactance of any other components.

It is suggested that a marginal oscillator be constructed in which:

1) the varicap be replaced by a mechanically variable parallel plate capacitor, to be modulated at the detection frequency(12),

2) the feedback loop used to maintain oscillation contain a frequency sensitive element that could compensate for the frequency dependent reactance changes of the other components,

3) the actual modulation waveform used be bidirectional, in order to minimize the effects of any residual amplitude modulation(13).

With careful construction it should be possible to build a frequency-modulated oscillator, along these lines of design, that is capable of excursions greater than 1% of the center frequency with almost undetectable amplitude modulation.

PROPOSITION V

The two most common types of oscillating detectors used in nuclear quadrupole resonance are the super-regenerative oscillator (14) and the marginal oscillator (13). The marginal oscillator is comparatively simple, and fairly easy to construct. There is no necessity of maintaining the critical balance conditions that are required in circuits employing cross coil and balanced bridge circuitry (11). Only the frequency of the tank circuit need be varied; no other reactive element need be changed(See Fig. P-5-1a). An alternative circuit which has seen comparatively little use has been proposed by Robinson (See Fig. P-5-1b).

In the Robinson circuit one uses a wide-band amplifier followed by a limiter. The voltage output from the limiter is fed back across the resonant circuit. If both the gain of the amplifier, and the output of the limiter are constant with frequency, there will be a change in the voltage output of the wide band amplifier when the sample is absorbing energy from the resonant circuit. A non-linear device, such as a diode, can be used to detect the change in radio frequency level.

The vacuum tube in a conventional marginal oscillator is run at a very low level, $\sim$ 1/10th of normal operation level. In this region of operation regeneration is fairly linear, and changes in loading of the oscillator due to resonant absorption are detectable

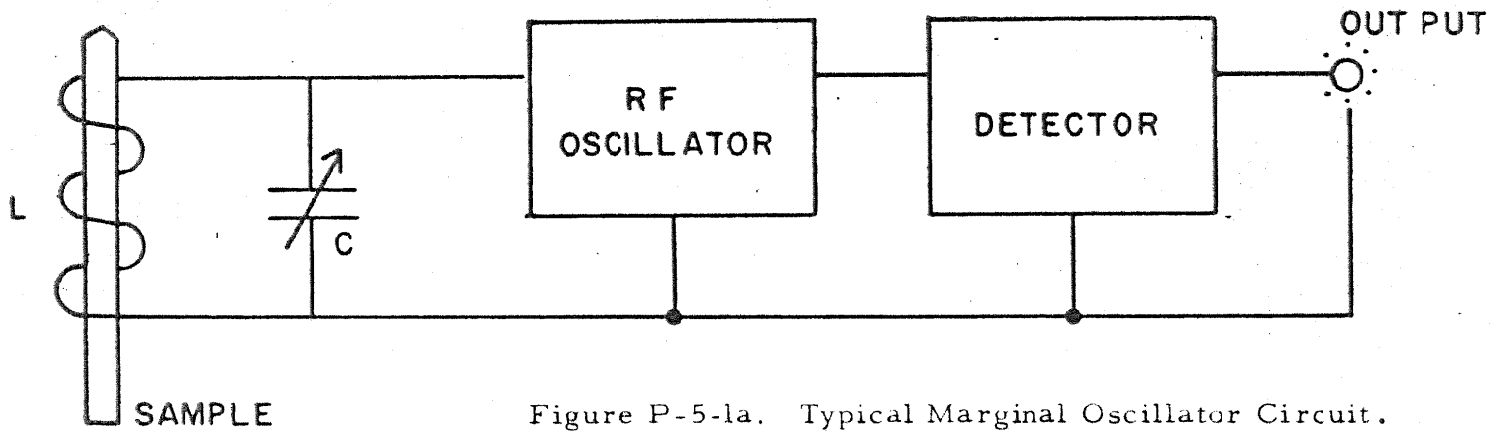

Figure P-5-1a. Typical Marginal Oscillator Circuit.

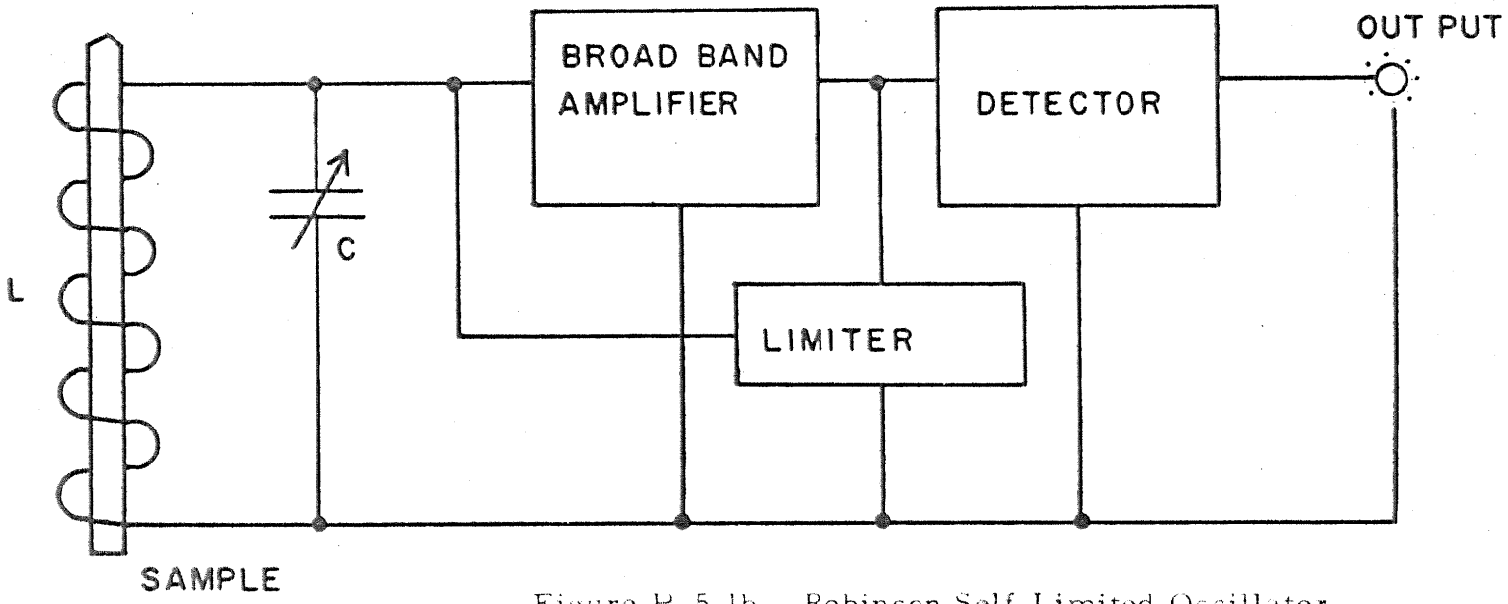

Figure P-5-1b. Robinson Self-Limited Oscillator.

due to a resultant decrease in level of oscillation. If the level of oscillation is increased, the operation of the tube becomes more and more non-linear, until the level of oscillation is primarily determined by tube characteristics. Under these circumstances the oscillator is very insensitive to the small changes in loading caused by sample absorption. In practice, there is also a lower limit to the level of oscillation imposed by the stability of the components used.

The principal advantages of the Robinson circuit arise from separation of the amplifier and limiter function. Since the limiting is done after amplification, at a fairly high level, there is in principle no lower limit to the level of voltage across the resonance coil. Likewise, high power levels may be used without loss in sensitivity, providing one has sufficient amplifier power available.

In his original paper (15) Robinson reported a self-limited oscillator, using three pentode stages of amplification, which could scan from 20 to 65 Mc/sec , with radio frequency voltage levels between 10 and 200 mv. Because of the limited gain-bandwidth products of vacuum tubes (ca. 200 for modern pentodes), the amplifier circuitry rapidly becomes more and more formidable as attempts are made to extend the frequency range.

The present proposal makes use of commercially available amplifier equipment. The proposed range of operation is between

ca. 200 Kc/sec to 200 Mc/sec (frequency limitation set by amplifier bandpass), with a radio frequency power level variable over a factor of 10^4. This wide range in power level should be useful for observation of saturation effects, etc.

The 500 Series of amplifiers made by Instruments for Industry (IFI) have the required bandbass with gains of 12 to 16 db. By cascading an IFI Model 510 Amplifier with a Model 500, we can obtain a power gain of 28 db. The two amplifiers in series will also provide the necessary phase inversion needed before the limiter stage. A vacuum tube which will serve as a limiter is the 6 AK5 , a pentode capable of operation up to frequencies of 400 Mc/sec (See Fig. P-5-2).

Operational Parameters: With a normal screen voltage, V_b, of 150 volts, the grid voltage, V_o, can vary from approximately 2 to 16 volts, and the tube will still act as a satisfactory limiter. This would correspond to radio frequency voltage levels in a range from about 100 to 1000 mv. As V_b is reduced to 25 volts, the range for V_o drops to about 0.25 to 2 volts, corresponding to a a range of radio frequency voltages between 10 and 100 mv. This range of voltages (10 to 1000 mv) would correspond to a change in radio frequency power level of approximately 10^4.

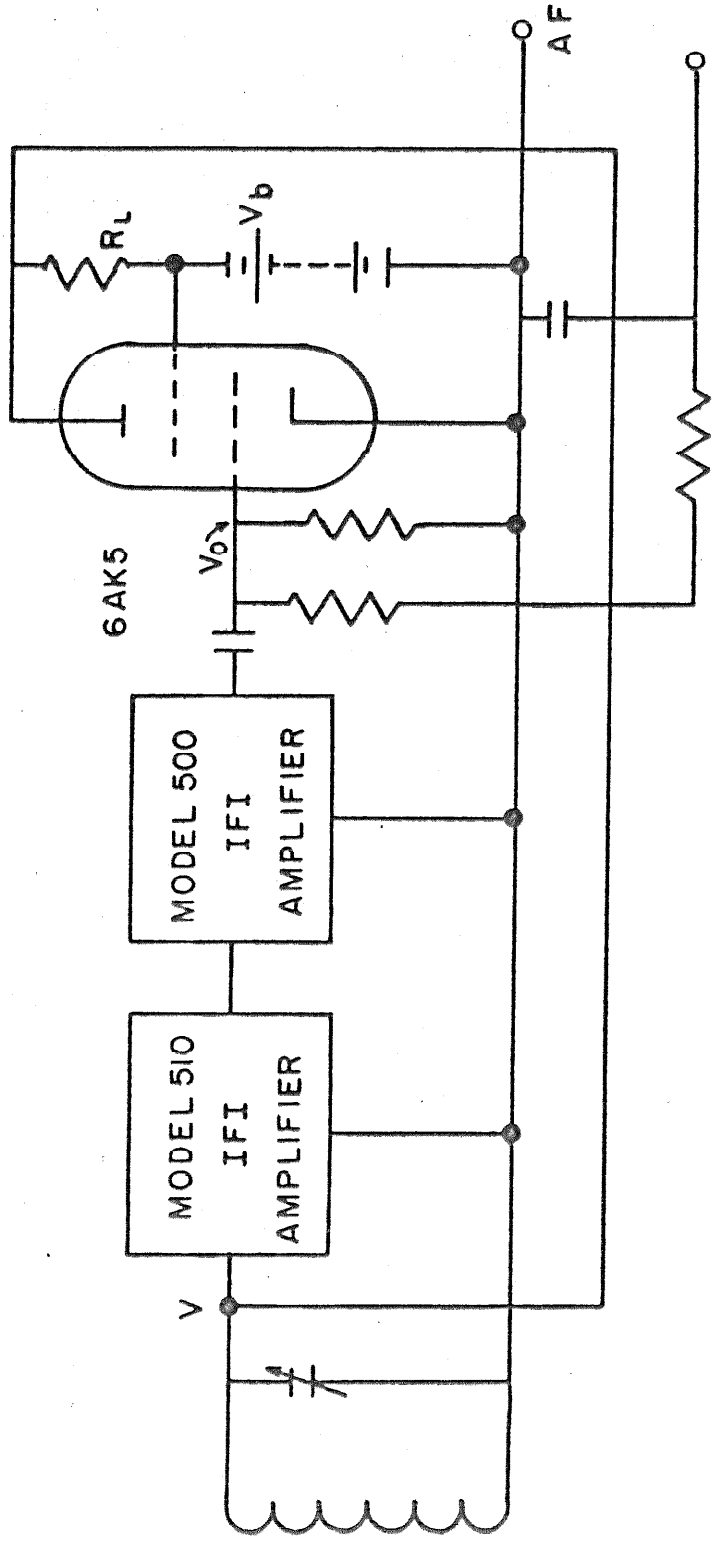

Figure P-5-2. Semi-Schematic of Proposed Self-Limited Oscillator.

PROPOSITION VI

The following proposal, made originally in 1960, is presented with some recent experimental data which is pertinent to the proposed study:

" The existence and determination of rotation barriers about single bonds has provoked much interest and discussion since the initial work of Kemp and Pitzer (16). Compounds such as dimethyl acetylene are of special interest because the barrier is very low, or, perhaps, zero. Using his bent bond theory Pauling (17) predicted a finite barrier of the order of 0.5 kcal/mole; with π-bonding the barrier would be < 0.00001 kcal/mole.

" Solid state nuclear magnetic resonance seems to offer the possibility of determining whether the barrier is nearly zero or very small. If, indeed, there is free rotation of the methyl group, and the matrix (e.g., solid argon) does not restrict the rotation, we would expect essentially all of the molecules to be in a state with the methyl group in its zeroth rotational state at 2^{o} K (see below). The possibility of negligible matrix interaction with the methyl group seems hopeful in view of the already observed istotropic rotation of substances such as the $NH_2\cdot$ and $CH_3\cdot$ radicals under these conditions (18, 19, 20).

" Because of the Pauli Exclusion Principle and from symmetry considerations, only the four symmetric nuclear spin functions would be allowed for the methyl group in its zeroth rotational state(21). Using these spin functions one could calculate the spectra of a polycrystalline sample.

" Alternatively, one might obtain the spectra of three equivalent protons; the theoretical line shape for this system has been calculated by Andrew and Bersohn (22). The would result from either a non-negligible internal rotation barrier, or a lattice interaction. An estimate of the latter might be obtained from performing a similar experiment with a compound such as nitromethane, where the internal barrier (o.oo6 kcal/mole) is known. "

RECENT EXPERIMENTAL WORK

Since the possibility of doing the above experiment hinges on a negligible interaction of the methyl group with the lattice, the following experimental results are presented.

Heller (23) has irradiated a single crystal of $CH_3CH(COOH)_2$ and obtained oriented $CH_3\dot{C}(COOH)_2$ radicals. The room temperature electron spin resonance spectrum of this radical showed the expected hyperfine interaction. Four lines, with intensity ratios

1:3:3:1, were observed. The spectrum at 77°K was unchanged. The spectrum at 4.2°K, however, showed a marked decrease in intensity for the center two lines, with line intensities of 1:1.5:1.5:1, interpreted as evidence of substantial population of only the lowest two rotational states of the methyl group causing the hyperfine interaction. If only the lowest state were populated, there would, of course, be four lines of equal intensity. This work indicates that any internal barrier or any lattice barrier is less than ~ 2 cm^{-1} ($\sim$0.006 kcal/mole).

Some work on inclusion compounds done here at Caltech (24) also indicates that even fairly large molecules, containing methyl groups, can be introduced into single crystals without restricting the rotation of the methyl group at temperatures as low as ~ 7°K (The compound was not investigated at lower temperatures). Thus, instead of polycrystalline spectra, it should be possible to do broad-line nuclear magnetic resonance on oriented molecules.

ROTATIONAL ENERGY STATES

The above estimate of the population of the rotational states is based on the following. The rotational energy levels of a methyl group about a C—C bond are given by the familiar formula:

$$E_k = \lambda k^2 = (h/8\pi^2 c I)\ k^2 ,$$

where h is Planck's constant, c is the velocity of light, and I

is the moment of inertia of the methyl group about the C — C bond. Using tetrahedral angles, and C — H bond distances of 1.09 A^{o} , one obtains λ = 5.3 cm^{-1}. The excitation energies are, therefore,

$$E_{0,\pm1} = 5.3\ cm^{-1}\ ,\quad E_{0,\pm2} = 21.2\ cm^{-1}\ ,\quad \text{etc.}$$

Hence, the statement that at 2°K the system would be almost entirely in its zeroth rotational state.

REFERENCES FOR PROPOSITIONS

1. C. Dean and E. Lindstrand, J. Chem. Phys., 24, 1114 (1956).

2. Benedek, Bloembergen, and Kushida, Bull. Am. Phys. Soc., Ser. II, 1, 11 (1956).

3. Kushida, Benedek, and Bloembergen, Phys. Rev., 104, 1364 (1956).

4. G. Watkins and R. V. Pound, Phys Rev., 89, 658 (1953).

5. Private Communication to H. M. McConnell from T. Cole and Kushida, both of Ford Motor Company.

6. See, e.g., Bridgman, The Physics of High Pressures, G. Bell and Sons, Ltd., London (1949).

7. Blosser and Young, Rev. Sci. Instr., 33, 1007 (1962).

8. C. A. Hutchison, Jr., and B. W. Mangum, J. Chem. Phys., 29, 952 (1958).

9. Radiation Laboratory Series, M.I.T., McGraw-Hill Book Company, New York (1948).

10. See Part II of this thesis.

11. See, e.g., Andrew, Nuclear Magnetic Resonance, Cambridge University Press (1958); Ingram, Free Radicals, Butterworths Scientific Publications, London (1958).

12. Kojima, Shimauchi, Hagiwara, and Abe, J. Phys. Soc. Japan, 10, 930 (1955).

13. The ideas discussed in Part I of this thesis, although particularly pertinent to magnetic field erasure, can be carried over to the case of frequency modulation with little modification.

14. See, e.g., Das and Hahn, Nuclear Quadrupole Resonance Spectroscopy, Academic Press, New York (1958).

15. F. N. H. Robinson, J. Sci. Instr., 36, 481 (1959).

16. Kemp and Pitzer, J. Am. Chem. Soc., 59, 276 (1937).

17. Seminar at Caltech, cf. Pauling, Proc. Natl. Acad. Sci., 44, 211 (1958).

18. Robinson, J. Chem. Phys., 30, 999 (1959)

19. H. M. McConnell, J. Chem. Phys., 29, 1422 (1958).

20. T. Cole, etal., Mol. Phys., 1, 406 (1958).

21. Herzberg, Infrared and Raman Spectra, 406 ff., D. Van Nostrand, Lancaster, Pennsylvania, 1949.

22. Andrew and Bersohn, J. Chem. Phys., 18, 159 (1950).

23. Heller, J. Chem. Phys., 36, 175 (1962).

24. O. H. Griffith, private communication.